AN ABSTRACT OF THE THESIS OF

ROBERT DOYLE WADDLE for the degree of MASTER OF SCIENCE

in CHEMISTRY presented on APRIL 21, 1989

Title: The Determination of Gasoline and Alkyl Benzenes in Aqueous Solution and the Development of a Remote Reaction Chamber for Fiber Optic Remote Sensing

Abstract approved: Redacted for Privacy

J. D. Ingle, Jr.

The development and optimization of a single-phase derivatization technique for small ring aromatics in water are presented. Also described are the design, optimization and application of a remote reaction chamber for fiber optic sensing.

Aqueous solutions of the major aromatic compounds in gasoline are derivatized to o-nitrosophenol-Cu complexes with a modified Baudisch reaction. The rate of formation of the complex is spectrophotometrically monitored at 310 nm and related to the concentration of benzene and alkyl benzenes present. The measured rate for aqueous gasoline samples is then related to gasoline concentration by estimating the relative aromatic composition of the gasoline sample. The technique provides a detection limit (DL) of 4×10^{-5} % (v/v) and 4×10^{-4} % (v/v) for benzene and gasoline, respectively. The response is linear to 0.01% (v/v) for benzene and 0.005% (v/v) for gasoline. The technique was successfully applied as a bench top method for detecting gasoline and alkyl benzenes, but due to the loss in reactivity of the reagents once mixed, the methodology was not suited for remote sensing

applications.

A remote reaction chamber (RRC) optrode was developed to facilitate in situ monitoring using derivatization techniques to form a luminescent product. The RRC optrode is a submergible chamber into which excitation radiation is input with one optical fiber and emission radiation is collected and directed to a photodetection system with another optical fiber. The RRC optrode allows for the isolation of a sample by applying a vacuum to a one-way exhaust valve. When the vacuum is applied the sample enters through a one-way intake valve and partially fills the internal chamber. After the vacuum is terminated, up to three reagents are injected with automated syringes through injection lines. Mixing of the sample and injected reagents is accomplished with a miniature stir driver and stir bar contained in the RRC optrode. The formation of a luminescent species results, and the intensity of the emitted radiation is related to the concentration of the analyte being studied.

The RRC optrode was developed and optimized for the determination of trace levels of Al(III) and Cr(VI). A modified method of standard addition was also developed for use with the RRC optrode and optimized for the Al(III) study.

Trace levels of aluminum are determined by measuring the rate of formation of the fluorescent chelate of Al(III) with 2,4,2'-trihydroxy-azobenzene-5'-sulfonic acid. This method provides a DL of 0.13 ng/mL and a linear dynamic range of four orders of magnitude using the RRC optrode. One of the reagent lines of the RRC optrode was configured to inject an Al(III) standard solution to implement in situ standard

addition measurements. Analysis of a tap water sample with external standards and the standard-addition procedure produced equivalent results.

Low concentrations of Cr(VI) in water were determined by monitoring the intensity of the chemiluminescence (CL) produced when Cr(VI) is mixed with a lophine-H_2O_2-KOH reagent system in the RRC optrode. This technique exhibits a DL of 11 ng/mL with a linear response up to 10 µg/mL.

THE DETERMINATION OF GASOLINE AND ALKYL BENZENES IN AQUEOUS SOLUTION AND THE DEVELOPMENT OF A REMOTE REACTION CHAMBER FOR FIBER OPTIC REMOTE SENSING

by

Robert D. Waddle

A THESIS

submitted to

Oregon State University

in partial fullfillment of
the requirements for the
degree of

Master of Science

Completed April 21, 1989

Commencement June 1989

APPROVED:

Redacted for Privacy

Professor of Chemistry in charge of major

Redacted for Privacy

Chairman of Department of Chemistry

Redacted for Privacy

Dean of Graduate School

Date thesis is presented April 21, 1989

Typed by Robert D. Waddle for Robert D. Waddle

DEDICATED TO

Mom and Dad

TABLE OF CONTENTS

LIST OF FIGURES

LIST OF TABLES

THE DETERMINATION OF GASOLINE AND ALKYL BENZENES IN AQUEOUS SOLUTION AND THE DEVELOPMENT OF A REMOTE REACTION CHAMBER FOR FIBER OPTIC REMOTE SENSING

INTRODUCTION

This research encompasses the investigation and development of remote, in situ monitoring techniques for determination of trace level contaminants. These remote sensing techniques involve spectroscopic analysis using fiber optics to transmit electromagnetic radiation to and from the sample. The basic design of a spectrometric remote sensing system is presented in Figure 1. This system includes a conventional radiation source, monochromators and/or filters, optical fibers, a detector, and a signal processing device. Excitation radiation of the desired wavelength is directed into the sample via an optical fiber. Depending on the orientation of the optical fibers, a specific constituent or group of constituents of interest is detected by its UV-visible absorption or fluorescence characteristics. The transmitted or fluorescence radiation is collected and directed by a second fiber to a wavelength selection and detection system. Chemiluminescence (CL) measurements are also possible and do not require excitation radiation. This technology allows the monitoring of a difficult to reach sample with the majority of the monitoring equipment in a convenient location. This methodology permits in situ monitoring of an aquifer or other type of sample and provides an efficient means to detect species in real time and to eliminate inaccuracies due to sampling and sample storage.

Remote analysis using fiber optics for chemical sensing is a

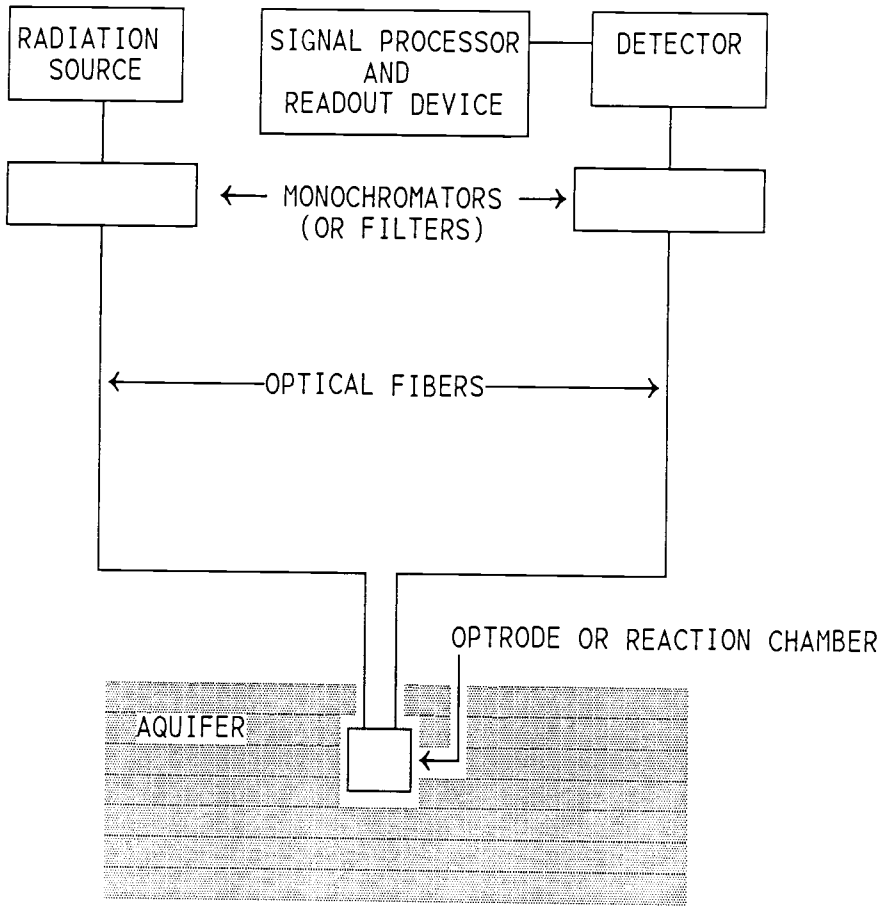

Figure 1. Instrumental scheme for the analysis of an aquifer using luminescence remote sensing via fiber optics.

rapidly growing field. Areas of research using these fiber optic sensors, often, called optrodes, have encompassed a variety of in situ as well as in vivo applications (1-6).

This thesis is divided into two parts. The first section is concerned with a study to determine the feasibility of developing an optrode to be used as a sensor to detect gasoline contamination in water. This method involves the derivatization of the significant aromatic component of gasoline into a chromophore which is active in the visible region of the electromagnetic spectrum. The in situ synthesis of a visible chromophore would allow spectroscopic detection of the analyte using fused silica fibers. The use of visible region wavelengths is highly desirable if not mandatory because UV radiation is highly attenuated even by the highest quality fused silica fibers.

The second section of the thesis addresses the development of a submersible reaction cell which isolates a small volume of sample in a small reaction chamber. The distal ends of the excitation and emission optical fibers of a fiber optic system are inserted into the sample chamber. After sample isolation, selective reagents are mixed with the sample in the cell. The introduced reagents result in the attachment of a fluorescent label to the analyte or the synthesis of a luminescent species related to the analyte which can be detected in the visible range. This reaction cell represents a new type of optrode and is denoted the remote reaction chamber (RRC) optrode. The mechanical logic of the RRC optrode introduces the capability of conducting bench top type analysis requiring reagent addition, stirring, and heating to in situ applications.

In this research the RRC optrode is developed and demonstrated

functional in two different applications. The first application of the RRC optrode involves a kinetics-based fluorometric determination of aluminum in aqueous solution. A detailed discussion of this methodology in a bench top application is presented by Campi (7). The application of in situ standard addition analysis is also demonstrated.

The second application is the determination of hexavalent chromium in water by lophine chemiluminescence (CL). The original CL analysis using conventional instrumentation was presented by Marino (8). A comparison study between conventional instrumentation and the RRC optrode/fiber optic system is also presented to characterize the collection efficiency of the fiber optic system.

These applications of the RRC are presented here as representative studies which demonstrate the general usefulness of this new methodology. The results suggest that the RRC greatly increases the possibilities of remote detection of chemical contamination in aqueous environmental samples as well as for monitoring of species in process control applications.

SPECTROSCOPIC DETECTION OF GASOLINE AND ALKYL BENZENES IN AQUEOUS SYSTEMS

HISTORICAL

Gasoline History

Gasoline has evolved from being nothing more than an unwanted by-product in the production of stove and lamp oils, lubricating oils and greases to an indispensable mainstay in less than a single human lifetime. Today the world consumes over 4.0×10^{11} L of gasoline every year.

Gasoline is primarily obtained from the distillate of crude oil (9). The crude oil is distilled and separated into several different boiling fractions by heating to 370-430° C in a fractioning tower. The distillation separates approximately 6 fractions; light naphtha, heavy naphtha, kerosene, light gas oil, heavy gas oil, and reduced crude (Table I). Only the light naphtha fraction is of high enough quality to be used initially as a component of finished gasoline. The heavier naphtha fractions can be catalytically reformed to a higher quality blending stock (reformate) by a separate process and then used as gasoline. This reforming process involves conversion of aliphatic and naphthenic (nonaromatic cyclic) compounds in the C_6-C_9 range into aromatics (dehydrogenation of cyclic paraffins and dehydrocyclization of straight chain paraffins C_6 or larger). Formation of these aromatics is desirable due to the higher octane number (quality rating) of the alkyl benzenes.

Table I. Breakdown of various principal crude oil fractions produced in the distillation of oil[a]

PRINCIPAL CRUDE-OIL FRACTIONS	APPROXIMATE BOILING RANGE, °C
Light Naphtha	0-100
Heavy Naphtha	100-200
Kerosene	200-250
Light gas oil	200-300
Heavy gas oil	300-400
Reduced crude	400-600

[a]Lane, J. C., "Gasoline and Other Motor Fuels", ECT 2nd ed., Vol II.

The term octane rating or octane number describes the quality of commercial gasoline samples or more specifically its antiknock quality. The octane scale was developed in 1926 by Graham Edgar of the Ethyl corporation as a yardstick for the measurement of gasoline quality. The scale involves a rating or octane number from 0 to 100, 0 being the poorest quality fuel and 100 the best (Figure 2). The standard used for zero on the scale is the straight chain hydrocarbon n-heptane which burns with considerable knock, while the non-knocking 2,2,4-trimethylpentane is the 100 standard. By blending these two hydrocarbons in varying percentages, Edgar was able to match the knock resistance of any gasoline sample. The knock of a fuel is measured electronically on a standardized single-cylinder, 4-stroke engine with a variable compression ratio.

Knock is believed to be the result of chemical reactions that begins almost as soon as the air fuel mixture enters the cylinder during the intake stroke. The mixture is progressively heated by the cylinder walls, by compression prior to the power stroke, and by burning gases after the spark plug fires. This heating causes the fuel hydrocarbons (HC) to undergo a series of cracking and oxidation reactions that convert them to unstable compounds prone to autoignition and instantaneous detonation. This instantaneous detonation (versus a smooth sweeping ignition front) over the piston top occurs too rapidly for the piston, connecting rod, and crankshaft assembly to respond, and the piston "rattles" in the cylinder during the explosion.

The antiknock capacity of a motor fuel is highly dependent upon the compression ratio of the engine it is used in. In the early half of the 21st century, the ON of motor fuels was not extremely critical

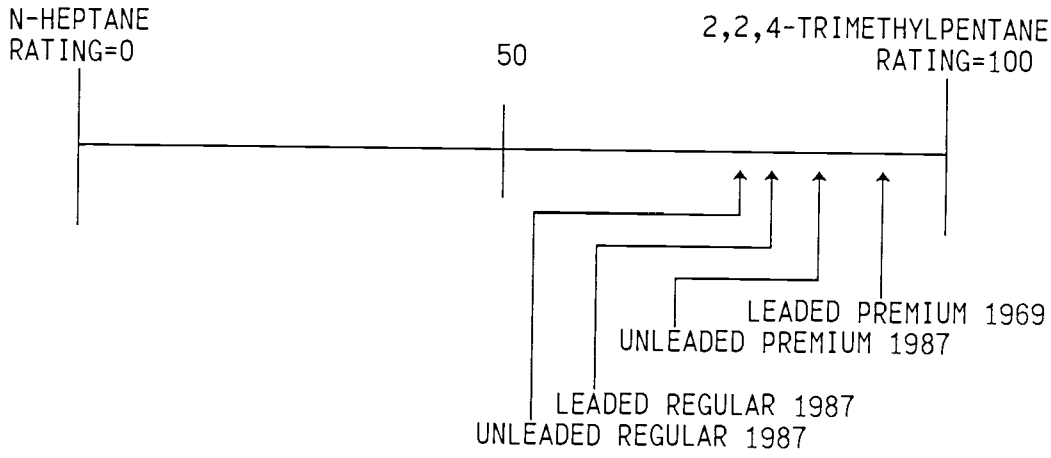

Figure 2. Octane rating scale showing the octane value of commercial gasoline samples (Shell Oil Co.) in relation to each other.

due to the low compression ratios of these internal combustion engines of approximately 5:1. In the 1960's engine performance and compression ratios increased dramatically. Compression ratios of 8:1 and even 12:1 became common. The increase in engine performance, created a need for high octane fuels. Gasoline manufacturers met this need by the reformation processes mentioned earlier and by the use of chemical fuel additives. The most efficient of these additives were quickly recognized to be the tetramethyl and tetraethyl lead compounds. These compounds, when mixed in small amounts with gasoline, offer a fuel with an enhanced ON which is extremely economical to manufacture.

Fairly early in the study of engine knock, it was recognized that the chemical structure largely determines the tendency to cause engine knock. Straight chain hydrocarbons are more prone to cause knock than are paraffins and olefins. Cyclic hydrocarbons or aromatic hydrocarbons are the least prone to cause knock (9). This knowledge brought about the use of certain hydrocarbons in chemical mixtures to provide high ON fuels for the consumer. These chemical mixtures incorporate additional quantities of alkyl benzenes such as toluene, the xylenes and other aromatic hydrocarbons which enhance the fuels antiknock character by virtue of their high ON as shown in Table II (10). Table III provides information on ON gains provided by different blending agents (9).

A gasoline engine produces a variety of pollutants including unburned hydrocarbons, carbon monoxide, and nitrogen oxides. The presence of tetraethyl lead adds lead compounds to the list of pollutants. In the early seventies, this pollution was addressed by restrictive legislation and catalytic converters were added to

Table II. Individual Research Octane Numbers (RON) for several small ring aromatics commonly used as gasoline additives[a]

COMPOUND	RON
Benzene	108
Toluene	112
Ethylbenzene	113
p-Xylene	114
m-Xylene	114
o-Xylene	100
Typical C_9 mix	103

[a]Peter, F. M., "The Alkyl Benzenes", National Academy Press, Washington D.C., 1981.

Table III. Numerical values representing the gain in octane value achieved from the 5% addition of the blending agent to a gasoline sample[a]

BLENDING AGENT	ON GAIN DUE TO 5% ADDITION[b]			
	UNLEADED REGULAR		LEADED REGULAR	
	RON	MON	RON	MON
Toluene	1.07	0.69	1.34	1.13
MTBE[c]	1.16	0.84	1.44	1.17
TBA[d]	0.78	0.63	0.70	0.85
Ethyl Alcohol	0.80	0.17	0.63	NEG

[a]Lane, J. C., "Gasoline and Other Motor Fuels:, ECT 2nd ed., Vol II.
[b]ON = octane number; RON = research octane number; MON = motor octane number
[c]MTBE = methyl tert-butyl ether
[d]TBA = tert-butyl alcohol

production vehicles to counter the problem. The catalytic converters change nonoxidized and partially oxidized compounds to more-highly oxidized and acceptable forms of exhaust. The platinum catalyst used in these converters is "poisoned" (made nonfunctional) by lead compounds; therefore, leaded fuels could no longer be used in automobiles equipped with these converters. At present all new cars are equipped with catalytic converters which excludes them from using lead additive fuels. Presently legislation is slated to take effect in the year 1990 which will ban the sale of leaded fuels entirely. Since the introduction of the converters, use of the alkyl benzenes and other aromatic hydrocarbon mixing agents has increased and will continue to increase as the lead compounds are completely phased out (11).

Gasoline Composition

The composition of gasoline varies dramatically from sample to sample, depending on several variables such as the geographical origin of the crude oil (Table IV) and the individual manufacturers specifications (regular, premium, unleaded, etc.). Table V shows the composition of several gasoline samples by major hydrocarbon group. Of particular interest here is the aromatic content of the samples which ranges from 40 to nearly 70% (12). Even though some gasoline samples have been shown to contain less than 10% aromatics (13), the aromatic content of a given gasoline sample is generally considerably higher (10, 12, 14).

The aromatics in gasoline are of such considerable interest because they are more toxic than the other constituents of gasoline.

Table IV. Composition of crude oil samples from various regions and countries[a]

COMPOUND	PERCENTAGE, BY SOURCE				
	LOUISIANA GULF	WEST TEXAS	VENE-ZUELA	LIBYA	IRAN
Naphtha at 66-149°C	13	18	10	17	15
Total C_6-C_8 aromatics					
in crude	1.1	1.79	1.85	1.0	1.80
in naphtha	8.5	11.0	18.5	5.8	12.0
Benzene					
in crude	0.15	0.18	0.15	0.07	0.19
Toluene					
in crude	0.45	0.51	0.60	0.37	0.56
C_8 aromatics					
in crude	0.50	1.10	1.10	0.56	1.05
Total C_6-C_8 naphthenes					
in crude	3.87	6.37	3.4	2.50	2.92
Benzene precursors					
in crude	0.67	0.97	0.50	0.55	0.65
Toluene precursors					
in crude	1.3	2.0	1.6	1.05	1.19
C_8 aromatics precursors					
in crude	1.9	3.4	1.3	0.90	1.08

[a]Lane, J. C., "Gasoline and Other Motor Fuels", ECT 2nd ed., Vol II.

Table V. Major component breakdown of several commercial gasoline samples[a]

TYPE	BRAND	CONCENTRATIONS (wt %)		
		SATURATES	OLEFINS	AROMATICS
LEADED REGULAR	A	50.3	3.3	46.4
	B	53.8	4.8	41.4
	D	38.8	7.5	53.7
UNLEADED REGULAR	A	42.0	14.4	43.6
	B	43.1	16.6	40.3
	C	21.4	10.7	67.9
	D	44.7	9.0	46.3
UNLEADED PREMIUM	A	32.7	3.9	63.4
	B	39.1	8.5	52.4
	C	37.6	3.4	59.0
	D	43.7	7.8	48.5

[a]Miller, R. L., J. Chromatogr., 264, (1983) 19-32

The aromatics are also much more spectroscopically active than the aliphatic fraction of gasoline and are therefore the main target of this research.

Gasoline In Groundwater

The storage of gasoline in underground tanks has been common practice since the development of gasoline. These tanks have commonly been fabricated out of steel and are accessed via steel fittings. As these steel tanks age, they become increasingly prone to leaks due to corrosion and other structural failures (15). These leaks lead to the contamination of the surrounding soils (unsaturated zone) and eventually the groundwater system (saturated zone).

Accidental leakage of petroleum products from underground storage tanks and pipelines is a major concern to the petroleum industry, federal and state governments, and to the informed public. Generally gasoline leaks from service station storage tanks are the most frequently reported source of groundwater contamination by gasoline (15). Such leaks are prevalent due in part to the installation of a large number of metal storage tanks during the post world war II building boom which have since lost their integrity due to corrosion.

Many case studies of groundwater contamination have been documented in the literature (16, 17). The problems associated with contamination are severe. These problems range from health risks associated with ingestion (10) of the alkyl benzenes to explosions in private residences due to gasoline fumes which have escaped from the water table into residential basements (16). Once a spill has

occurred, the effects of this leak are potentially long lasting. Contamination of soils and groundwater as long as 20 years after the spill are documented (16).

The problems discussed above indicate that the early detection of gasoline contamination in groundwater supplies is of paramount importance. Early detection of the leaks via analysis of groundwater samples is one means of preventing major long term problems encountered with gasoline leaks in subterranean storage equipment.

Part of the work in this thesis is concerned with the detection of gasoline in groundwater. Specifically the detection of gasoline and alkyl benzenes in aqueous systems using spectrophotometric methods is addressed. Presently methods of detection and analysis are almost solely limited to gas chromatography (GC) and gas chromatography-mass spectrometry (GC-MS) (10, 18, 19). Infrared analysis has also been applied in a very limited number of cases (20, 21). These methods of analysis involve sample collection from the suspect site, and in most cases, sample preparation of some type is required before analysis. This sample handling introduces the possibility of sample contamination due to human handling errors. Given the volatility of many of the constituents of gasoline, the loss of analyte in the sampling process or during storage before analysis is also highly likely. The problems associated with current methods of analysis as mentioned above, as well as the expense involved with analytical methods such as GC-MS, indicate the need for a rapid, relatively inexpensive method to detect the approximate level of gasoline contamination in groundwater.

Remote Spectroscopic Analysis

For in situ monitoring of groundwater the detection of a specific constituent or group of constituents of gasoline in aqueous solution can be accomplished using UV and visible absorption or fluorescence spectrometry. For UV and visible detection of gasoline, the constituents which are of the most interest are the alkyl benzenes.

Characteristic spectra of the alkyl benzenes are based on transitions in the far and near UV regions of the electromagnetic spectrum. The transitions of several alkyl benzenes along with their corresponding molar absorptivities and wavelengths are presented in Table VI. The transitions in the near-UV region are more interesting in the detection of gasoline in aqueous systems than those transitions in the far-UV region due to selectivity. Transitions in the far-UV region involve high energy electronic transitions characteristic of sigma bonds; therefore, the number of species which absorb in this region is extremely large. For UV and visible applications, the determination of gasoline via detection of the alkyl benzene fraction which absorbs in the 200-300 nm wavelength region is preferred.

Aromatic hydrocarbons are usually fluorescent in the UV-VIS region of the spectrum (22). The π electrons can be promoted to π^* antibonding orbitals by absorption of near-UV radiation without disruption of bonding. Furthermore, π to π^* transitions in most aromatic hydrocarbons are strongly allowed ($\epsilon_{max} \simeq 10^3$ to 10^4). Finally the small ring aromatic compounds have reasonable fluorescence quantum yields (22). For example, toluene has a fluorescence quantum efficiency of 0.23 in hexane.

Table VI. Electronic transitions responsible for the spectroscopic activity of several small ring aromatic compounds[a]

COMPOUND	ELECTRONIC TRANSITIONS	λ_{max} (nm)	ϵ_{max} (L/mol-cm)
Benzene	Aromatics π-π^*	180	60,000
	"	200	8000
	"	255	215
Toluene	Aromatics π-π^*	208	2460
	"	262	174
Phenol	Aromatics π-π^*	210	6200
	"	270	1450

[a]Silverstein, R. M., "Spectrometric Identification of Organic Compounds", 4th ed., Wiley and Sons, New York.

Fiber Optic Limitations

Currently fiber optic applications for analysis in the UV region are limited by the low transmission of quartz fibers for UV radiation. The attenuation of even the best fused silica fibers in the UV region (λ = 266 nm) is 400-500 dB/km vs. 40 dB/km or less for visible light (λ = 514 nm). This large attenuation of UV radiation represents a 95% loss in incident radiation over 25 m of fused silica fiber. Transmission losses of this magnitude require high power radiation sources such as lasers in order to conduct in situ type analysis in the UV region. Working instrumentation has been developed using UV radiation from the fourth harmonic of a portable Line-Lite YAG Lite Nd: YAG laser producing 0.1 mJ at 266 nm with a pulse duration of 10 ns at 5 Hz for in situ analysis of groundwater (23, 24). In this case detection of gasoline contamination at the sub-part per billion level is possible over a fiber length of 50 m. The usefulness of a portable laser system is limited however by the large cost of producing and maintaining such an instrument.

One goal is to develop in situ analysis instrumentation using current fiber technology and a low cost, stable radiation source which can withstand the adversities encountered in field monitoring. To apply lower power radiation sources to this problem, radiation of longer wavelengths which is less attenuated by transmission through optical fibers must be used. Obviously this presents a problem in the analysis of gasoline which is a mixture of hydrocarbons that are almost entirely transparent to energy at wavelengths longer than 280 nm.

Derivatization of Alkyl Benzenes

One approach to solving this problem is found in chemical derivatization of one or several components of the sample of interest. The derivatization approach involves conversion of the analyte which is spectroscopically active in the UV region of the spectrum to a new compound with visible absorption or fluorescence activity. A requirement of the derivatization scheme is that it involve simple single phase chemistry which would be suitable for in situ applications.

The derivatization is performed within a small reaction vessel or cell located at the distal end of an optical fiber system called an optrode. As previously mentioned, applications of optrode systems for in situ analysis have been studied extensively (1-6). However no chemical system could be found in the literature that has been used for the analytical determination of benzene or alkylbenzene via the selective derivatization to a visible chromophore.

An evaluation of standard synthetic methods involving aromatic ring chemistry, namely aromatic substitution (electrophilic, free-radical, nucleophilic), reveals that most of this chemistry is not suitable for in situ analysis. These reactions require special conditions such as heating, product separation, and non-aqueous reaction media to achieve minimal product yields. Of these reactions however, the most suitable are based on free-radical substitution (25).

Aromatic substitution involves the addition of a substituent to the ring which would offer a site of reactivity for further derivatization. The addition of a reactive substituent to the ring

such as a hydroxyl, amine, or nitro group would in itself cause a shift in the spectroscopic activity of the chromophore to longer wavelengths to a small degree (26). However, this initial substitution does not produce a species which can be detected in the visible region. The substitution must then be followed by additional derivatization of the analyte. An example of this would be the free-radical addition of a hydroxyl group to the aromatic ring using Fenton's reagent (27). The resultant phenol could then react with a fluorescent labelling agent such as dansyl chloride. Dansyl chloride is a standard labelling compound for fluorescent detection of aromatic hydroxyls and amines in liquid chromatography (28, 29). The chemistry and feasibility of this procedure is considered in detail later.

The Baudisch Reaction

As discussed above, most methodology for the derivatization of small ring aromatics involves multiple synthetic steps which greatly increases the difficulty of conducting the synthesis in an optrode. For simplicity, a one step synthetic method to a visible chromophore is desirable. Such a method was developed about 47 years ago by O. Baudisch (30). Using aqueous hydroxylamine hydrochloride, hydrogen peroxide, and a metal catalyst, he conducted the one-step synthesis of the o-nitrosophenols from benzene and substituted benzenes. The o-nitrosophenol was then isolated as a stable complex using Cu(II) ion. The copper complex produced is a bright red colored aqueous solutions and exhibits several absorption bands ranging from 200 to 600 nm as shown in Figure 3. The synthesis, now known as the Baudisch

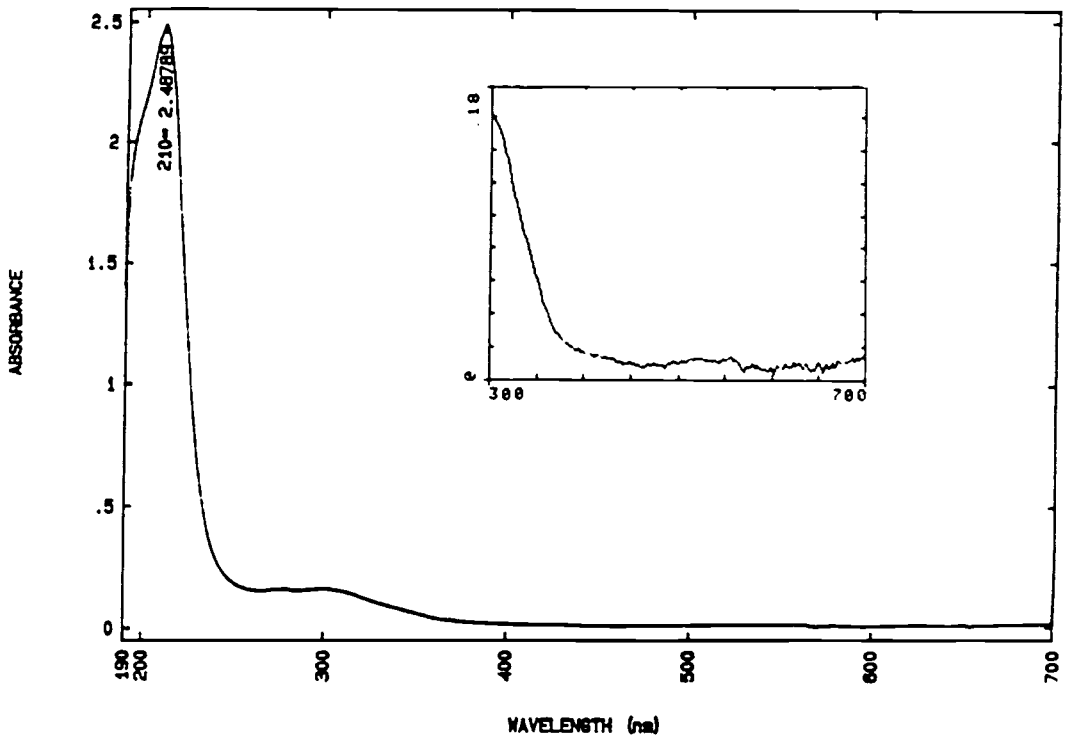

Figure 3. The UV-visible spectrum of the Baudisch reaction product, Cu(II)-o-nitrosophenol complex, in aqueous solution. 10 µL neat benzene in 3 mL reaction solution of 0.60 M H_2O_2, 0.107 M H_2NOH, 33 mM Cu(II).

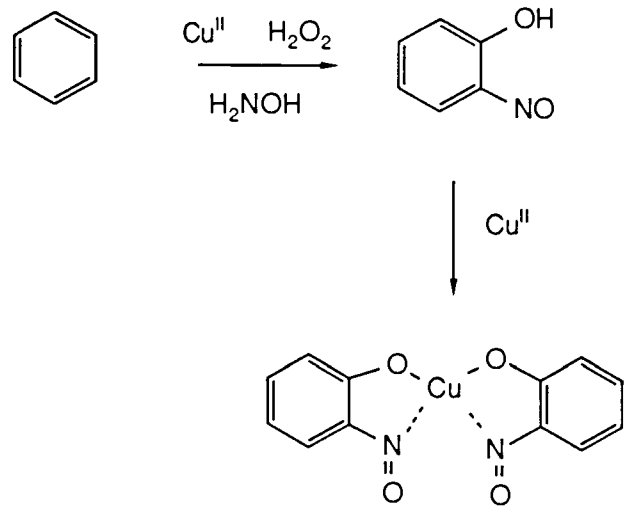

Figure 4. The Baudisch Reaction (synthesis of o-nitrosophenol)

reaction, is outlined in Figure 4.

Since the initial work by Baudisch, several workers have studied the mechanism of the reaction. Kazuhiro et. al. (31, 32) concluded that the formation of phenolic compounds is essential in Baudisch reactions of aromatic hydrocarbons. This hydroxylation of aromatic hydrocarbons proceeds through the decomposition of hydrogen peroxide catalyzed by Cu(I) ion as shown in Figure 5. Additionally, nitrosation through the formation of a Cu(II)-hydroxylamine complex and a phenoxy ion was proposed as the essential requirement for the predominantly ortho nitrosohydroxylation.

The Baudisch reaction was originally used as a synthetic pathway in producing o-nitrosophenol as stated earlier. It has also used as a method for detecting metal ions which form o-nitrosophenol complexes in the place of copper (33). The reaction has the potential of being a means of in situ derivatization of alkyl benzenes and gasoline. It is the purpose of the first part of this thesis to determine the feasibility of applying the Baudisch synthesis in the detection of trace amounts of alkyl benzenes.

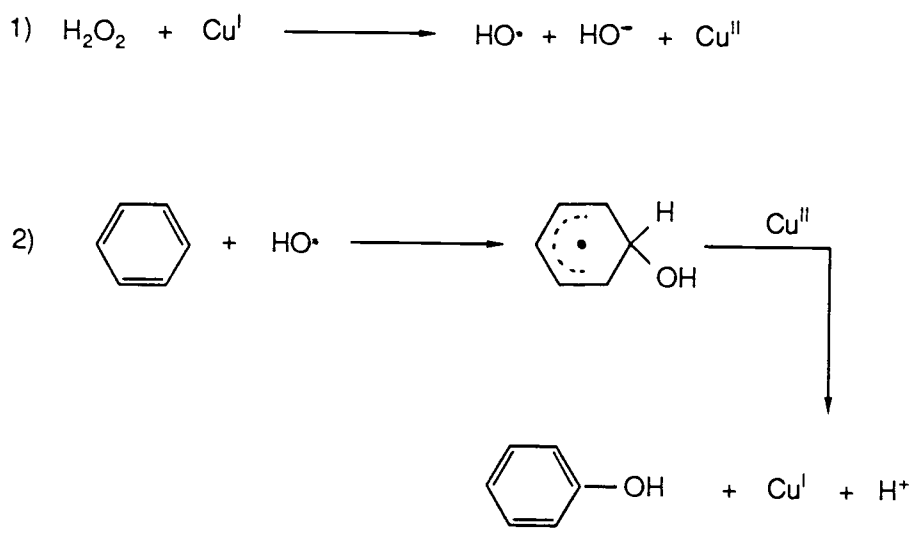

Figure 5. The proposed reaction mechanism for the first step of the Baudisch reaction.

EXPERIMENTAL

Solution Preparation

All aqueous solutions were prepared using double-deionized water from a Millipore Milli-Q (MP) system fed by house deionized water. All glassware was cleaned with 50/50 (v/v) MP water/HNO_3 and rinsed with MP water. All chemicals used were reagent grade.

Stock aqueous solutions of aromatic compounds for study using the Baudisch reaction were prepared in the highest concentrations possible as limited by the solubility of the compound (Table VII). The aqueous aromatics solutions were prepared and stored in the glass volumetric flasks, sealed with parafilm and refrigerated when not in immediate use. Solutions of hydroxylamine hydrochloride (EM Science), stabilized hydrogen peroxide (Spectrum Chemical), and $CuSO_4 \cdot 5H_2O$ (Mallinckrodt) were prepared at various concentrations as needed during the reagent optimization experiments (Table VII).

Gasoline solutions were prepared from commercial fuel samples purchased from a local Shell Oil Company service station. All fuel samples were Shell Super Unleaded 2000.

Measurement Scheme

All absorption studies were performed on a Hewlett-Packard 8451A single-beam diode array spectrophotometer. All fluorescence studies were conducted on a Varian SF-330 spectrofluorometer. In both instruments a standard fused silica fluorescence cell with a 1-cm

Table VII. Concentrations of reagent and analyte stock solutions for the Baudisch reaction

Stock Aqueous Aromatic Solutions	% (v/v)
Benzene	0.1
Toluene	0.01
Xylene	0.01
Gasoline	0.01

	H_2O_2 (M)	$[H_3NOH^+]$ (M)	$CuSO_4 \cdot 5H_2O$ (M)
Initial	4.5	4.5	0.045
After Optimization	3.6	0.65	0.10

pathlength was utilized.

Addition of all solutions with volumes of 1 mL or less to the sample cell was accomplished using fixed-volume Eppendorf pipets. For volumes greater than 1 mL, a Gilson Pipetman variable volume pipet was used. Reagents and samples were mixed in the cell using a magnetic micro-stir bar driven by a miniature stirring motor which was mounted below the cell in the diode array spectrophotometer.

In the reagent optimization scheme, the following timing sequences for the adding, mixing, referencing and measuring the absorbance of the solutions were used.

Timing Sequence I

1) Add Cu(II), hydroxylamine, and hydrogen peroxide solutions to the cell with stir motor on. 2) Start timer at point of hydrogen peroxide addition. 3) Mix for five minutes then add the aqueous analyte solution. 4) Mix further for 10 s, take a spectrophotometric reference and then measure within 10 s followed by sequential measurements every minute for fifteen minutes. Measurements were taken with a 1-s integration time.

Timing Sequence II

Same as timing sequence one except a 1 min mixing time replaces the 5 min mixing time.

Initial reaction rates are calculated by fitting the absorbance versus time data of each reaction with a linear regression program on an HP 11C hand held calculator. The data points for the first five minutes of each analysis sequence are used in the regression

calculation to approximate the initial reaction rate.

RESULTS AND DISCUSSION

Absorption and Native Fluorescence Study of Gasoline and Alkyl Benzenes

Initial studies were conducted on the absorption and native fluorescence of gasoline and several alkyl benzenes which represent primary components of gasoline. Figure 6 shows the individual absorption spectra of benzene, toluene, the xylenes and gasoline in ethanol. For these spectra, the solvent was ethanol rather than water so that high enough concentrations could be used to obtain good quality spectra. The absorption spectra in water are similar to those in ethanol except that the bands are shifted slightly to shorter wavelengths. The two major absorption bands of gasoline can be attributed to the presence of these small ring aromatic compounds. The most intense absorption band for gasoline and the alkyl benzenes is centered at the 210 to 220 nm region. This band in the UV region of the spectrum would be the band of choice for gasoline analysis in absorption measurements in a system with little or no interferences. However, as stated earlier, this region of the spectrum is occupied by absorption bands from an enormous number of spectroscopically active compounds which could cause large interference problems. The second absorption band in the 240 to 280 nm wavelength region is slightly better suited for absorption measurements due to its longer wavelength but is still subject to considerable interference by other species active in this region.

The dependence of native fluorescence signal on the concentration

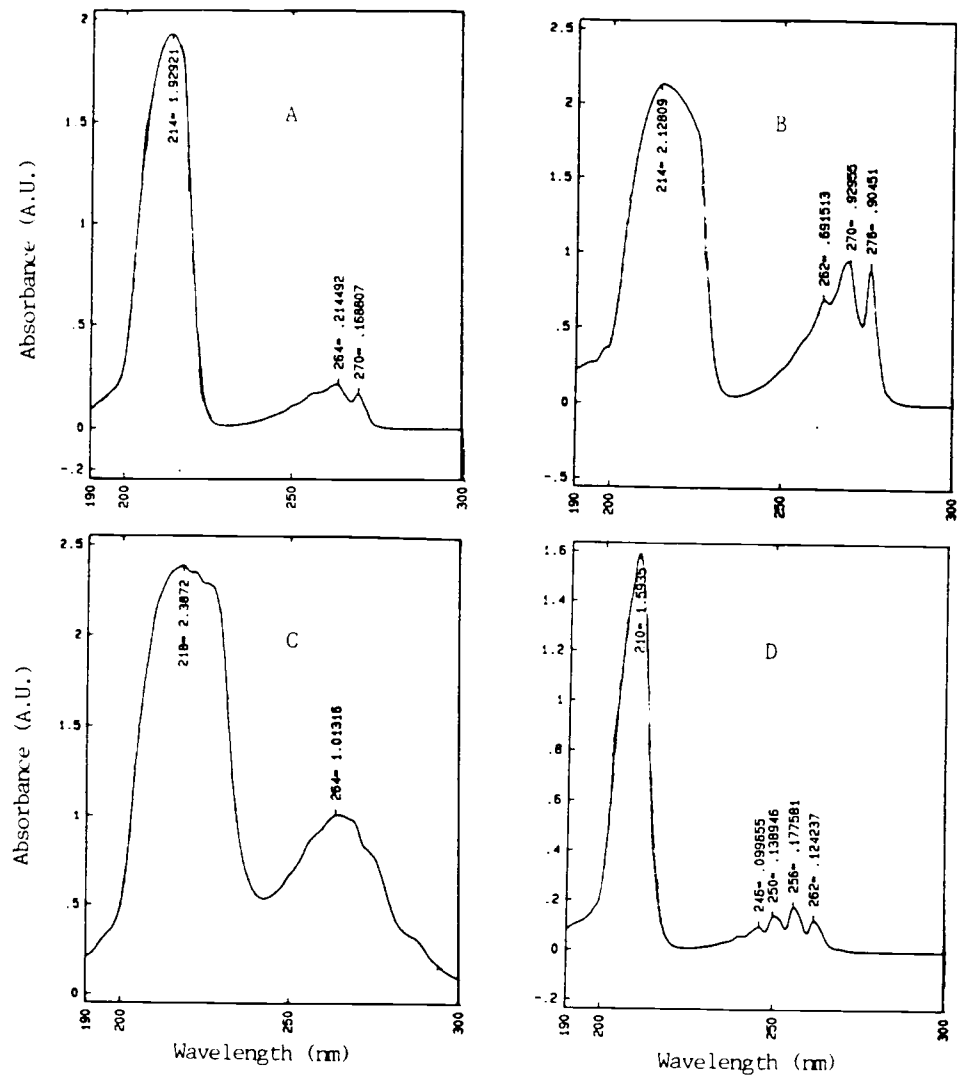

Figure 6. Absorption spectra of several alkyl benzenes and gasoline in 0.33% (v/v) ethanol solutions.
A = Toluene, B = Xylene, C = Gasoline, D = Benzene

of gasoline in water is presented in Figure 7. An excitation wavelength of 215 nm was used and the emission was monitored at 335 nm. No emission signal was observed using excitation energy in the 240-260 nm wavelength range. A linear response is observed over the gasoline concentration range of 1 to 10 μg/mL. Once again short wavelength analysis is subject to large interferences and is not suitable for fiber optic applications even though selectivity is improved by using fluorescence.

Feasibility Study of the Baudisch Reaction

The conventional scheme for the Baudisch reaction includes a petroleum ether extraction of the o-nitrosophenol followed by distillation and finally mixing with aqueous Cu(II) to form the stable Cu complex (30). This type of multi-step derivatization is not suited for in situ analysis as needed for an optrode reaction cell. Initial studies were directed at evaluating the feasibility of conducting the Baudisch synthesis in aqueous solution, in a single step, thereby eliminating the need for extractions. Benzene was the reaction substrate.

Bench top studies of the Baudisch reaction were performed using 4 mL of 30% (v/v) H_2O_2, 1 g of benzene, 4 g of hydroxylamine hydrochloride, and 2 g of $Na_2NH_4[Fe(CN)_5NH_3]\cdot 5H_2O$ as outlined in the original synthesis (30). The reaction was run in a beaker which contained all aqueous reagents and also a layer of chloroform to extract the product. The reaction was allowed to proceed with mild stirring. Within 1 hr the chloroform layer turned a distinct green

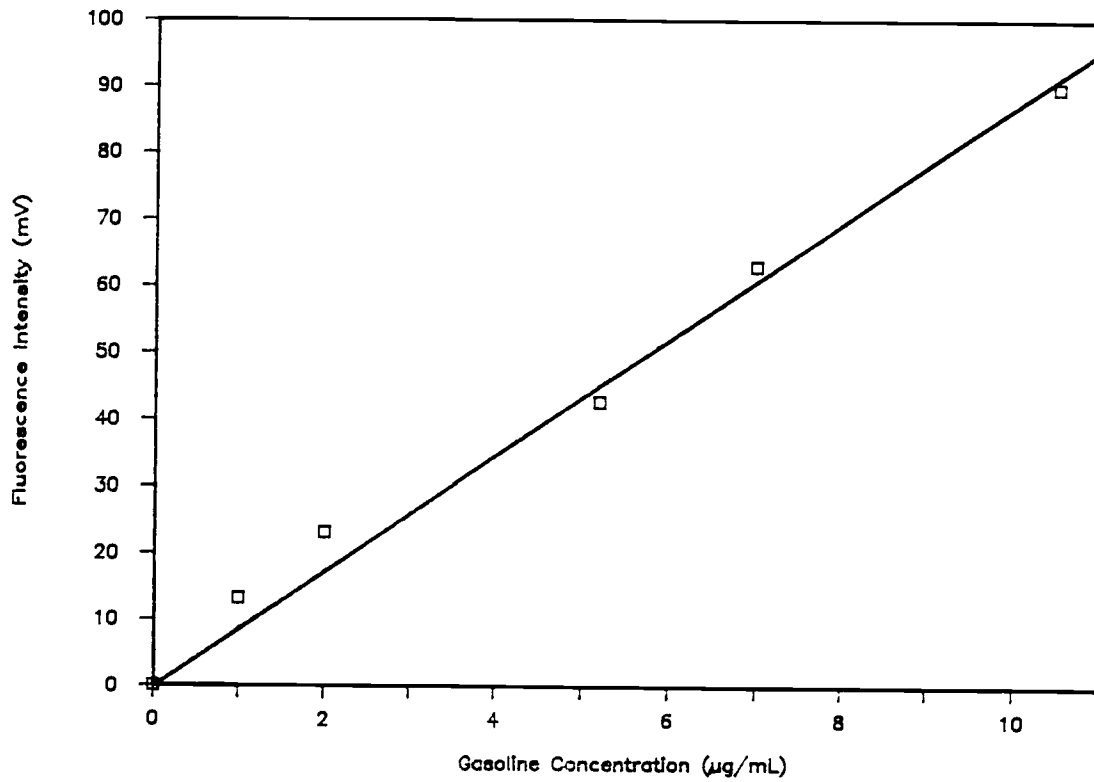

Figure 7. Fluorescence calibration curve for aqueous gasoline. Measurements were taken with emission and excitation bandpasses of 20 and 10 nm, respectively, and with a 4-s time constant.

color which is attributed to the expected product, o-nitrosophenol. The color was stable for several hours. The reaction was not carried any further to form the Cu(II)-o-nitrosophenol complex which would require distillation.

Next, the reaction was conducted with the same reagent concentrations in a fused silica optical cell without the organic layer. This reaction was monitored spectrophotometrically over the 280 to 600-nm range for a period of 24 hours. As with the two phase procedure, a green colored product was formed. The absorbance of the solution increased dramatically in the 300-nm to 400-nm range and to a lesser extent at longer wavelengths. This study demonstrated that the Baudisch synthesis of o-nitrosophenol was possible in a single phase system without organic extraction of the product.

Baudisch Reaction Reagent Optimization for the Single Phase System

To optimize the reaction rate of the Baudisch reaction under single phase conditions and to maximize the detectability to small ring aromatics, namely benzene, reagent concentration optimization studies were conducted. The three reagents involved in the optimization scheme are aqueous solutions of hydroxylamine hydrochloride, hydrogen peroxide, and Cu(II) ion. $CuSO_4$ was used in place of $Na_2NH_4[Fe(CN)_5NH_3]\cdot 5H_2O$ as the catalyst for the hydroxylation step. Maruyama et. al. demonstrated that $CuSO_4$ is a more effective catalyst than $Na_2NH_4[Fe(CN)_5NH_3]\cdot 5H_2O$ in aqueous systems (34, 35). A univariant optimization scheme was adopted where the concentration of only one reagent was changed while the other two were held constant. In each

case neat benzene was added in 10-μL aliquots.

Different reagent concentrations in the final reaction mixture were achieved by adding varying volumes of the reagent stock solutions. There is a rapid change in absorbance between 300 and 400 nm as mentioned earlier with an absorption maximum at 310 nm. The progress of the reaction was monitored at 310 nm because this wavelength yielded the greatest change in absorbance per unit time.

Table VIII summarizes the results from 20 different experiments where the reagent concentrations are varied. The reaction-rate curves for the five sets of reaction conditions which yielded the largest reaction rates are plotted Figure 8. As can be seen in Table VIII, the final reaction mixture volume for the first 10 reactions varied from 3.03 to 3.52 mL. This volume change was a result of using a constant volume of Cu(II) solution and adding varying amounts of H_2O_2 and H_2NOH. In order to hold the final cell volume constant the volume of Cu(II) solution added was varied in reactions 11 through 20. With this procedure, the concentration of Cu(II) ion varied from 34 to 44 mM. Further experimentation showed that this small change in the concentration of Cu(II) ion has little or no effect on the reaction rate in this concentration range.

In a separate experiment, the dependence of the rate on Cu(II) concentration in the cell was studied and the results are summarized in Figure 9. The total volume of the reaction mixture in the cell was held constant by adding 0.5 mL of 0.65 M hydroxylamine, 0.5 mL of 3.6 M hydrogen peroxide, 1 mL of 0.01 % (v/v) benzene and 1 mL of Cu(II) of variable concentration. The rate is independent of the Cu(II) concentration when the concentration of Cu(II) is greater than 30 mM.

Table VIII. Reagent concentrations in the reaction rate optimization scheme[a]

Rxn #	Cu^{2+} (mM)	Cu^{2+} Vol(mL)	H_2NOH (mM)	H_2NOH Vol(µL)	H_2O_2 (M)	H_2O_2 Vol(µL)	Rxn Mixture Vol(mL)	Rate[c] (A.U./min)
1	45	3.0	7.2	10	0.015	10	3.03	0.0125
2	45	3.0	7.0	10	0.073	50	3.07	0.0422
3	45	3.0	6.9	10	0.14	100	3.12	0.0615
4	45	3.0	6.9	10	0.28	200	3.22	0.0627
5	45	3.0	6.1	10	0.64	500	3.52	0.0705
6	45	3.0	35	50	0.015	10	3.07	0.0190
7	45	3.0	69	100	0.014	10	3.12	<0.005
8	45	3.0	35	50	0.072	50	3.11	0.0110
9	45	3.0	69	100	0.071	50	3.12	0.0105
10	45	3.0	134	200	0.069	50	3.21	<0.005
11	42	2.79	71	100	0.15	100	3.00	0.0505
12	39	2.59	143	200	0.30	200	3.00	0.0868
13	36	2.39	215	300	0.45	300	3.00	0.0750
14	40	2.64	108	150	0.30	200	3.00	0.0828
15	38	2.54	108	150	0.45	300	3.00	0.116
16	37	2.44	108	150	0.60	400	3.00	0.158
17	35	2.34	108	150	0.75	500	3.00	0.209[b]
18	37	2.49	143	200	0.45	300	3.00	0.120[b]
19	36	2.39	143	200	0.60	400	3.00	0.138[b]
20	34	2.29	143	200	0.75	500	3.00	0.150[b]

[a]Concentrations are in cell; 10 µL of neat benzene in each reaction.
[b]Bubbles in reaction cell made absorbance readings difficult.
[c]Rates are not blank corrected.

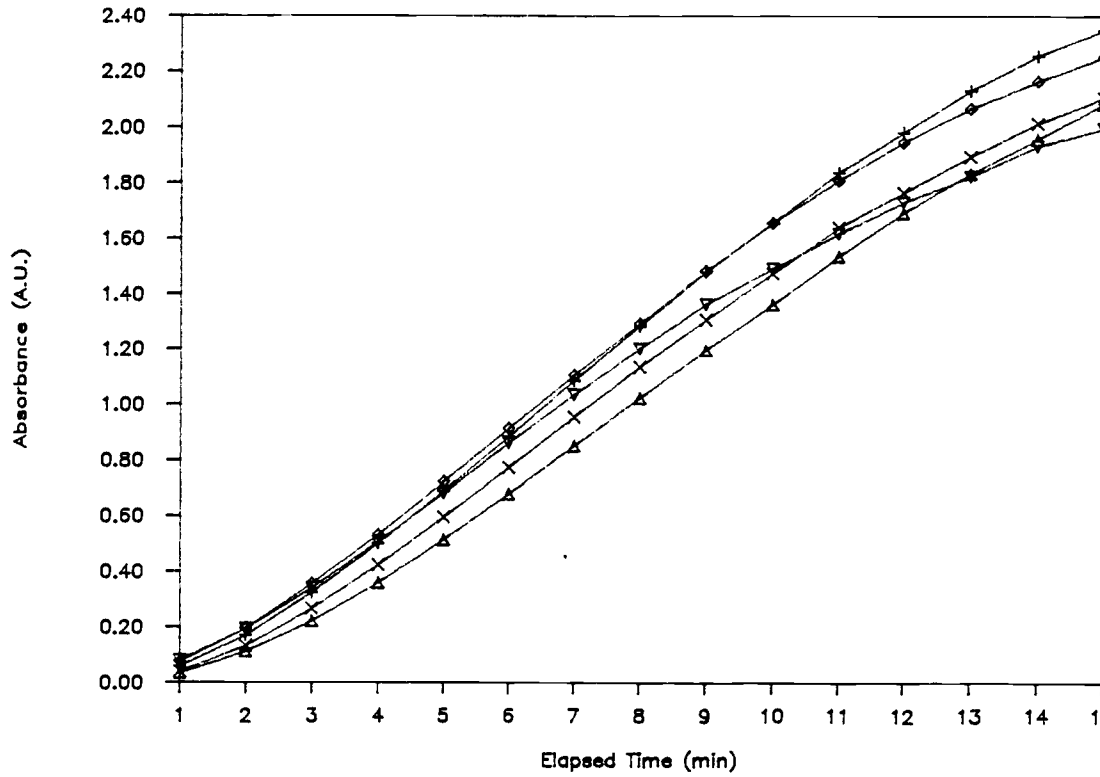

Figure 8. Reaction rate curves for the five best reaction conditions in the optimization scheme. The reaction was monitored at 310 nm. □ rxn #15, + rxn #16, ◇ rxn #17, △ rxn #18, x rxn #19, ▽ rxn #20.

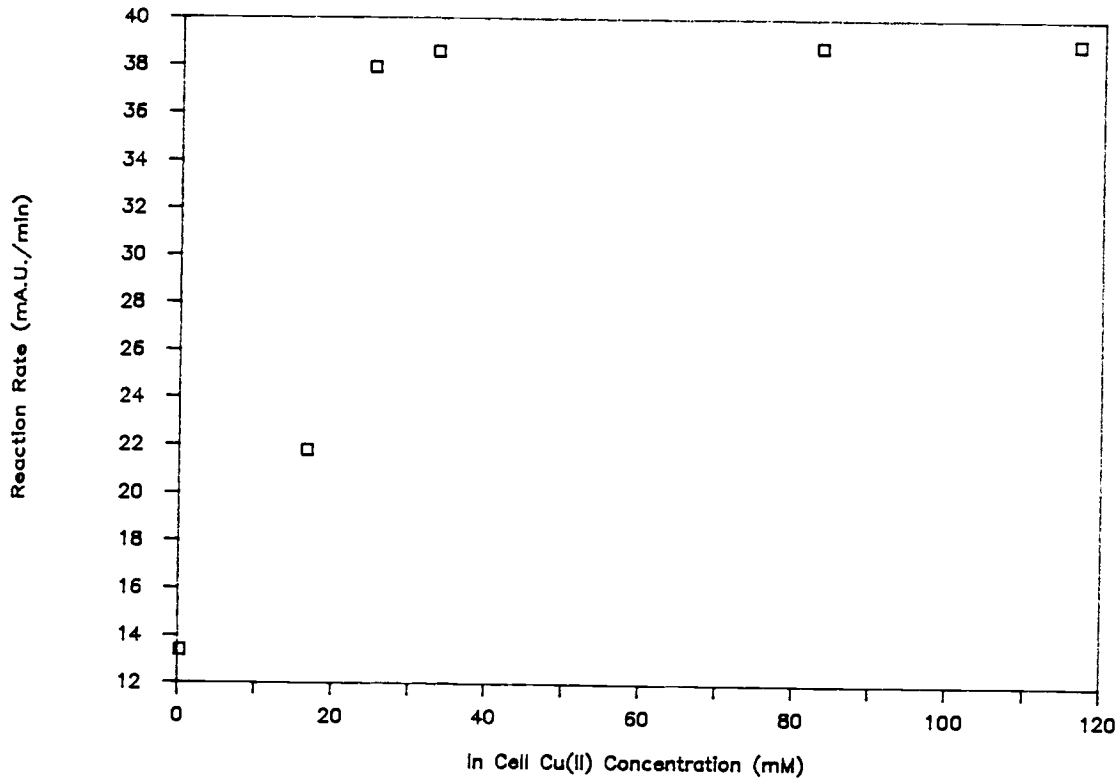

Figure 9. Effect of Cu(II) concentration on the reaction rate. Cell concentrations; 0.60 M H_2O_2, 0.11 M H_2NOH.

Based upon these data and for convenience, a 1-mL aliquot of 0.1 M Cu(II) was used in further studies. This provides a Cu(II) concentration of 33 mM in a 3-mL final reaction mixture.

In the reagent optimization scheme, the concentration ratio of hydrogen peroxide to hydroxylamine hydrochloride proved to be extremely influential on the reaction rate. If $[H_2O_2]/[H_2NOH]$ is too small, the rate of the modified Baudisch reaction becomes very small or negligible as evidenced by reaction conditions #7 and #10 in Table VIII. The lower reaction rate is attributed to the reduction of hydrogen peroxide by an excess of hydroxylamine. This outcome supports the conclusions of Maruyama et. al. that the initial and rate limiting reaction step in the Baudisch synthesis is the hydroxylation of the aromatic system. The hydroxylation is accomplished via a free radical mechanism involving hydrogen peroxide and a catalytic amount of Cu(I) as discussed earlier. This step of the synthesis leads to the production of phenolic compounds which absorb in the 270 to 310 nm wavelength range where the reaction progress is monitored in this work.

The data in Table VIII show that for fixed Cu(II) and H_2NOH concentrations, the reaction rate increases with increasing H_2O_2 concentration. This is demonstrated clearly by the rates for reactions 14 through 17 which are plotted in Figure 10. However, at H_2O_2 concentrations of 0.750 M and greater, the evolution of gas bubbles in the reaction cell prevents acquiring reliable absorption data. This bubbling problem was used to establish the concentration limit of H_2O_2 to be 0.60 M for further studies.

The next step in the optimization was to determine the hydroxylamine concentration which provided the best reaction rate. A

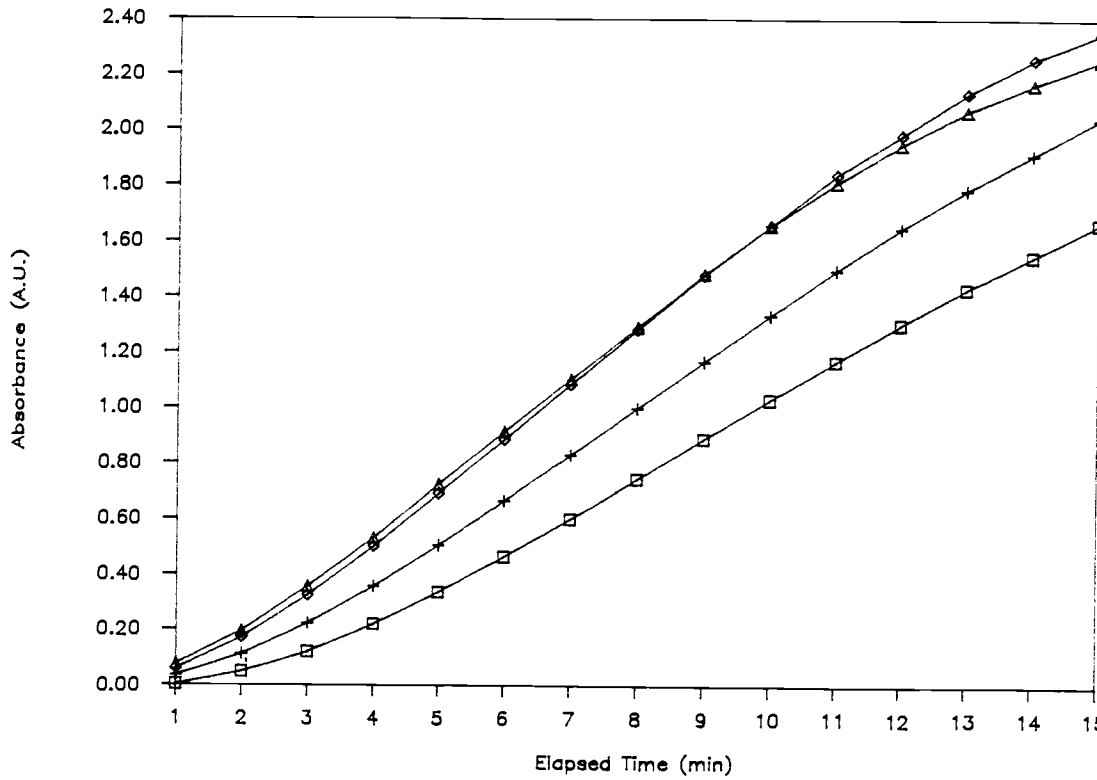

Figure 10. Effect of H_2O_2 concentration on reaction rate. Cell concentrations: Cu(II), > 33 mM; H_2NOH, 0.22 M. $[H_2O_2]$ = □ 0.3 M, + 0.45 M, ◇ 0.60 M, △ 0.75 M.

cell concentration of 0.11 M hydroxylamine for which $[H_2O_2]/[H_2NOH]$ = 5.4 provided the fastest reaction rate without bubbling. With a lower ratio, the rate of the Baudisch reaction decreased as shown in Figure 11. As noted earlier this decrease in reaction rate is attributed to the reduction of hydrogen peroxide by hydroxylamine.

Based upon the data presented above, the optimum reagent concentrations are 0.60 M hydrogen peroxide (0.5 mL of 3.6 M), 0.11 M hydroxylamine hydrochloride (0.5 mL of 0.65 M), and 33 mM Cu(II) (1 mL of 0.1 M). A sample volume of 1 mL is used to provide a total cell volume of 3-mL. These concentrations and volumes of reagents and samples are used in all future studies.

A final aspect of the Baudisch reaction optimization to be considered is the timing sequence of reagent addition and mixing. Up to this point all reactions were run under timing sequence I outlined in the experimental section. A series of experiments were conducted using 1 mL of a 0.01% (v/v) standard benzene solution which gave a good response with the reaction condition established up to this point in the experimental work. The reaction was run using mixing times of 0, 1, 2, and the standard 5 min. The results shown in Figure 12 indicate that a mixing time of approximately 1 min is optimum for the modified Baudisch reaction and this mixing time was used in all further studies.

Calibration Curve and Detection Limit for Benzene

A calibration curve with the optimized reagent concentrations constructed for aqueous benzene samples is shown in Figure 13. Nonlinearity is obvious over the three orders of magnitude range of

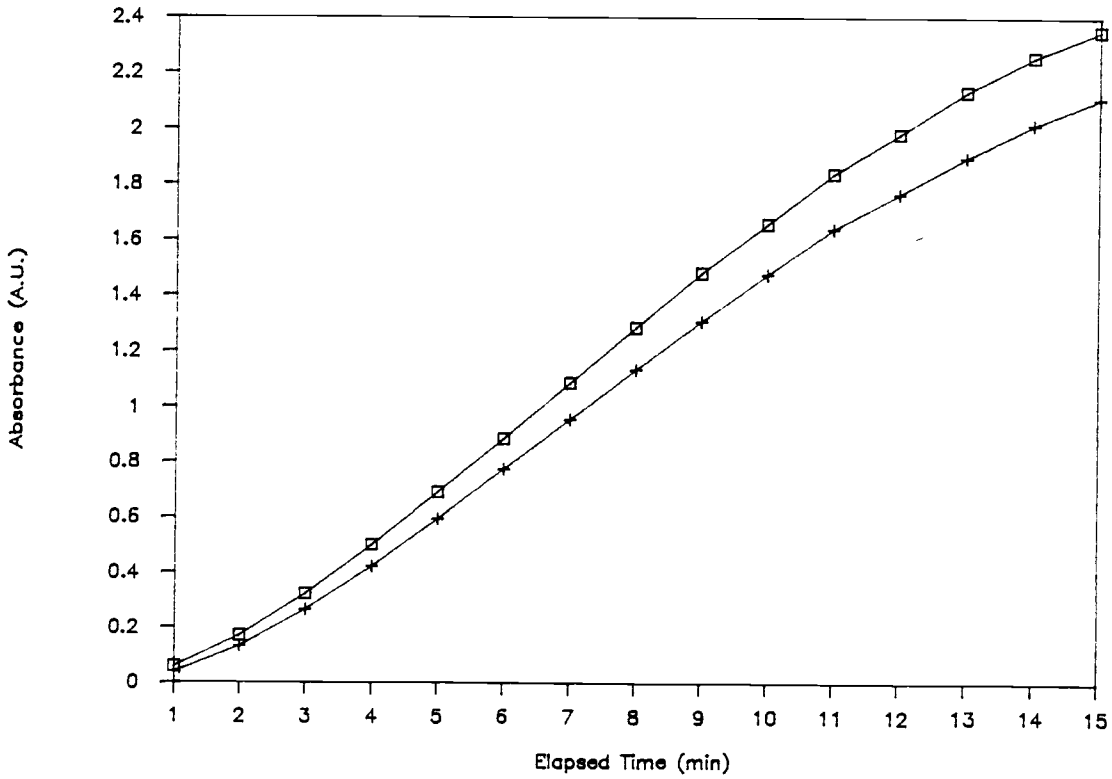

Figure 11. Dependence of reaction rate on the ratio of H_2O_2 to H_2NOH. □ $[H_2O_2]/[H_2NOH]$ = 5.4 (Rxn #16); + $[H_2O_2]/[H_2NOH]$ = 4.2 (Rxn #19).

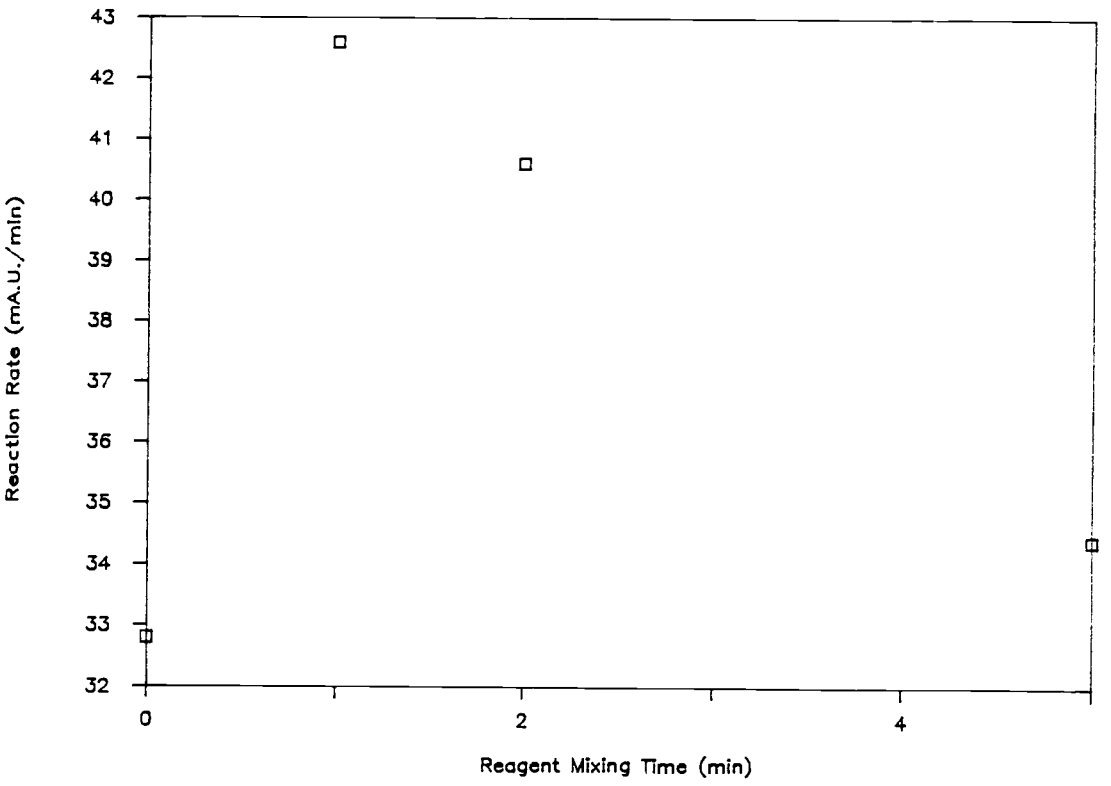

Figure 12. Dependence of the reaction rate of Baudisch reaction at various reagent mixing times before the addition of the analyte.

benzene concentration plotted. A second calibration plot over two orders of magnitude shown in Figure 14 does however demonstrate good linearity from 0.01% (v/v) benzene to the zero intercept.

The data points in Figure 14 are the mean of three runs. The means and standard deviations (SD) for the benzene standards and the blank are provided in Table IX. As can be seen only moderately good precision is attainable using the modified Baudisch reaction with the percent relative standard deviation (RSD) ranging from 2 to 6. The SD in the analyte rate is greater than that of the blank rate. This suggests that the precision of the rate measurements is limited by the irreproducibility in the reaction conditions from run to run. The detection limit (DL) calculated as the ratio of twice the blank standard deviation (Table IX) to the slope of the calibration curve (4.58 (A.U./min)/(% (v/v) benzene)) is 4.4×10^{-5} % (v/v) benzene.

Baudisch Reaction Results Using Alkyl Substituted Benzenes

The aromatic composition of typical gasoline fuels is predominantly alkyl substituted benzenes such as toluene and the xylenes (12-14). In determination of gasoline in water using the Baudisch reaction, it is then important to test the reaction efficiency using alkyl substituted benzenes as substrates. Table X summarizes the effects of alkyl substitution on the reaction rate of the Baudisch reaction. These data demonstrate that the rate decreases with increasing substitution. However, the reaction rate is decreased only 50% relative to benzene such that the detection limit for the major alkyl benzenes in gasoline is within about a factor of 2 of that of

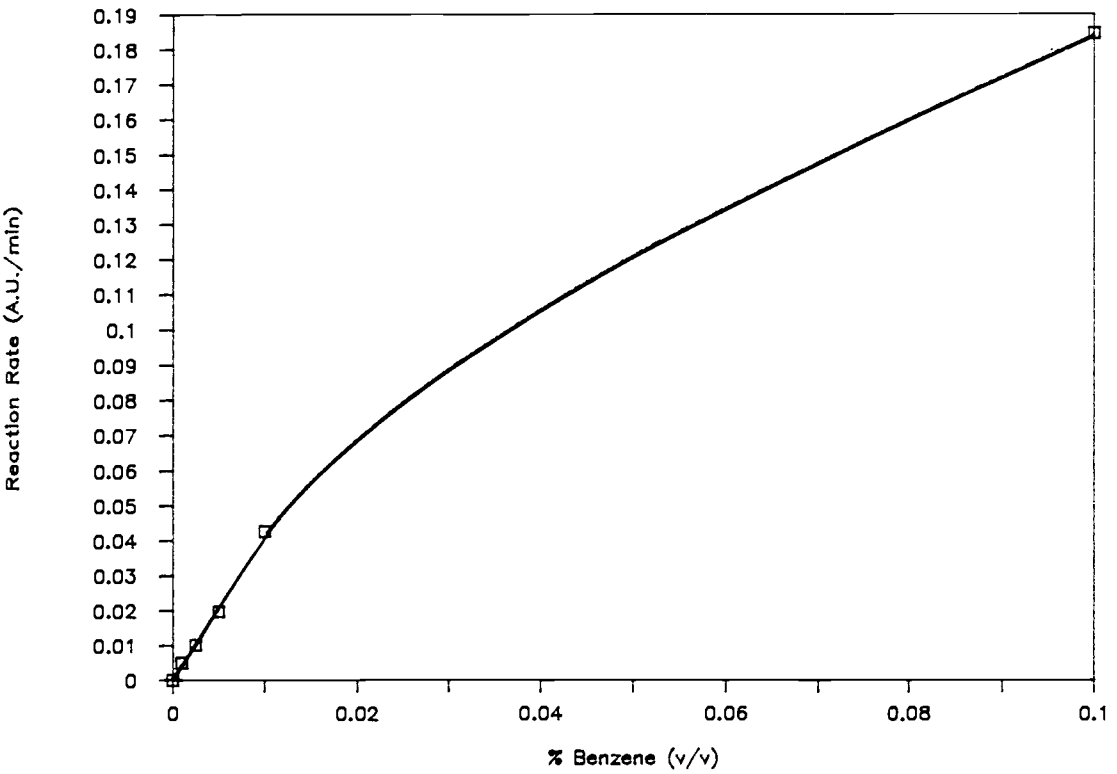

Figure 13. Calibration curve for benzene from 0.0 to 0.1% (v/v) benzene. 0.60 M H_2O_2, 0.11 M H_2NOH, 33 mM Cu(II).

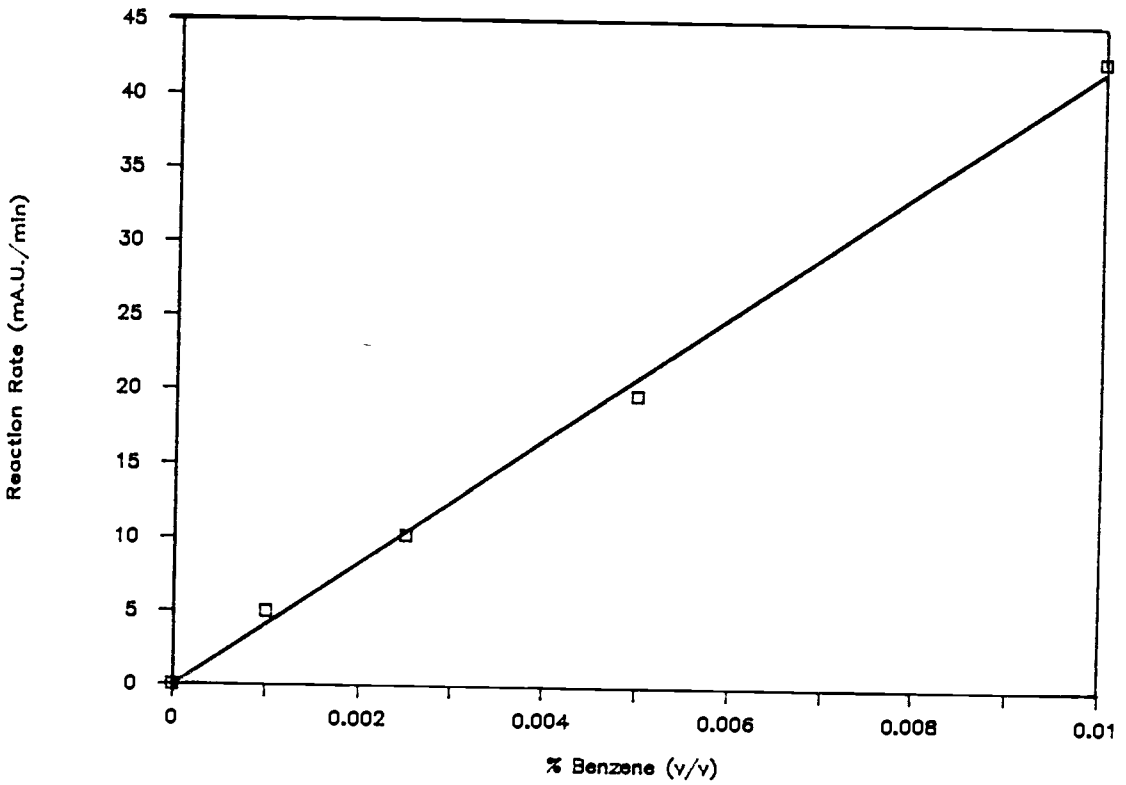

Figure 14. Calibration curve for benzene from 0.0 to 0.01% (v/v) benzene. 0.60 M H_2O_2, 0.11 M H_2NOH, 33 mM Cu(II).

Table IX. Reaction rate data for the Baudisch reaction calibration curve

% (v/v) BENZENE	REACTION RATE[a]		
	Mean	Std. dev.	RSD (%)
0.01	0.0420	0.002	5
0.005	0.0195	0.0004	2
0.0025	0.0100	0.0002	2
0.0001	0.00487	0.0003	6
BLANK	-0.00020	0.0001	

[a]A.U./min, n=5

Table X. Effect of alkyl substitution on the reaction rate of the Baudisch reaction

Compound[a]	# of Substituents	Reaction Rate[b]		% of Benzene Rate
		Mean	Std. Dev.	
Benzene	0	0.0364	0.0013	100
Toluene	1	0.0230	0.00003	63.2
Xylenes	2	0.0166	0.0012	45.6

[a]All standards 0.01% (v/v)
[b]A.U./min, n = 5

benzene.

The Detection of Gasoline in Water Using the Baudisch Reaction

Standard aqueous solutions of gasoline ranging from 0.01 to 0.001% (v/v) were analyzed in triplicate with the established optimum reagent concentrations and timing sequence. The data obtained in these experiments are provided in Table XI and are plotted in Figures 15 and 16. Nonlinearity is obvious above 0.005% (v/v) gasoline in Figure 15. However, a good first order fit is shown in Figure 16 where the plot encompasses the narrower range of 0.0 to 0.005% (v/v) gasoline. Reasonable precision (RSD $\leq$ 5%) for the reaction was obtained at all gasoline concentrations studied. The detection limit for gasoline as calculated from the ratio of twice the blank noise (Table XI) to the slope of the calibration curve (0.47 (A.U./min)/% (v/v) gasoline) is 4.2×10^{-4} % (v/v) gasoline.

The total aromatic fraction of the gasoline sample can be estimated from the response factors and composition of the aromatics present in gasoline. The response factor (RF) is simply the ratio of the calibration slopes of substituted aromatics to the calibration slope of benzene. As shown earlier toluene and the xylenes which are the major aromatic component of gasoline (14) are less reactive in the Baudisch reaction than benzene (Table X) giving response factors of 0.63 and 0.46, respectively. For typical gasoline, the toluene fraction of the aromatic component of gasoline is estimated to be 55% and the xylene and benzene fractions are 44% and 1%, respectively (14). From these data the mixed aromatic response (MAR) is calculated

Table XI. Data for the calibration curve for the detection of gasoline

% (v/v) GASOLINE	REACTION RATE[a]		
	Mean	Std. Dev.	RSD
0.01	0.00327	0.0001	3%
0.005	0.00230	0.00001	0.4%
0.0025	0.00120	0.00006	5%
0.001	0.00061	0.0001	2%
BLANK	-0.00020	0.0001	

[a]A.U./min, n = 5

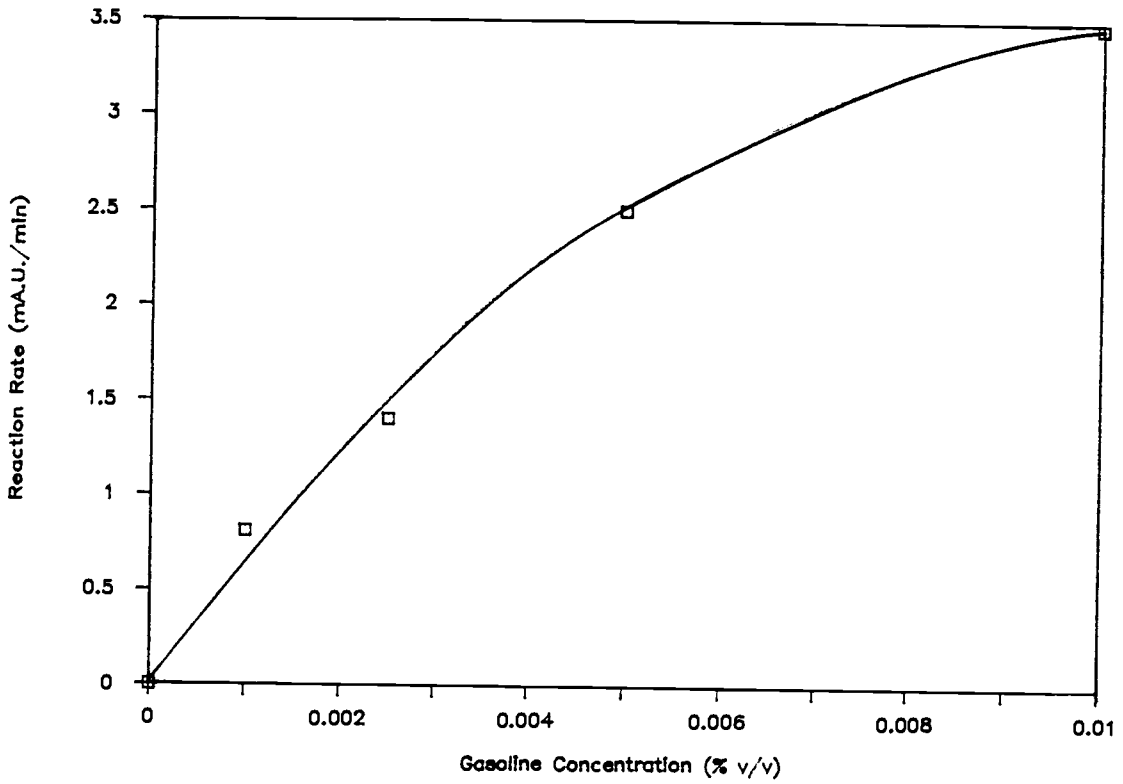

Figure 15. Calibration curve for the detection of gasoline using the Baudisch reaction (0.0 to 0.01% (v/v) gasoline). Data plotted with blank correction.

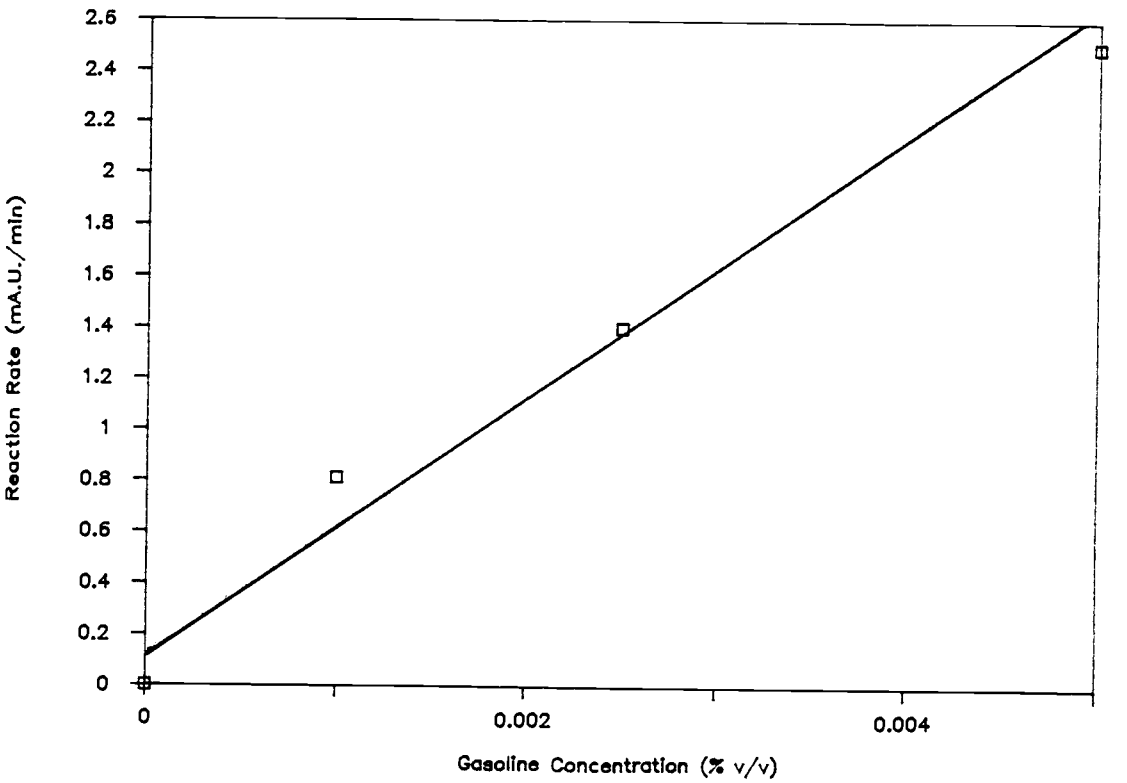

Figure 16. Calibration curve for the detection of gasoline using the Baudisch reaction (0.0 to 0.005% (v/v) gasoline). Data plotted with blank correction.

using Equation 1.

$$MAR = \Sigma[(\%\ Aromatic)_i \times (RF)_i] \qquad (1)$$

From the above percentages and RF factors and equation 1, the MAR is 54% or the aromatic fraction provides 54% of the rate of a gasoline for which the aromatic fraction is only benzene. Multiplying the slope of the calibration plot for benzene by this response correction gives a value of 2.47 A.U./min. The ratio of the gasoline calibration slope to the aromatic corrected slope represents an aromatic fraction in the gasoline sample of 19%. A 19% aromatic fraction is somewhat lower than the 30 to 60 % reported by some for an unleaded premium fuel (12, 13).

Gasoline samples also contain small amounts of tri (2%) and tetra-substituted (0.5%) benzenes (12, 13). From the trend seen in Table X the RF factor for the higher substituted aromatics would be expected to be less. The effect on the MAR would be minimal because of the low percentages of the higher substituted compounds present.

The Feasibility of Using the Baudisch Reaction for Remote Sensing for Extended Time Periods

A major concern for remote sensing applications using optrode systems is the operating lifetime of the reagents. Ideal conditions would allow the optrode to remain operative anywhere from a few days to a month without reagent replenishment.

To test the reagents used in the Baudisch reaction for long term stability, a single solution containing optimum concentrations of all

three reagents was prepared. The reaction was run with the single reagent solution immediately after preparation with the standard mixing time sequence, then at half hour intervals for two hours, and finally after 24 hours. Figure 17 shows that the reactivity of the reagents in the Baudisch reaction decrease rapidly with time. After 30 minutes the reaction rate is 5 times lower that that seen with freshly mixed reagents and 7 times lower after 24 hours.

The loss in reactivity of the reagent mixture is probably due to the oxidation-reduction reaction taking place between hydrogen peroxide (the oxidizing agent) and hydroxylamine hydrochloride (the reducing agent). This reaction depletes the reagents rapidly in the absence of the aromatic substrate.

This loss in reactivity is not acceptable for long term in situ monitoring. Clearly the Baudisch reaction can only be used in an optrode designed such that the H_2O_2 and H_2NOH are stored separately and combined immediately before the analysis.

Investigation of Other Derivatization Techniques

As previously mentioned the addition of substituent to the benzene ring such as a hydroxyl group would offer a site of reactivity for further derivatization. The free radical hydroxylation of benzene using Fenton's reagent and others are well represented in the literature (27, 36-40). With the formation of the phenol or cresol, fluorescence detection using dansyl chloride could be possible (28, 29). Upon further investigation this method of detection is not suitable for in situ single step analysis. The detection of the

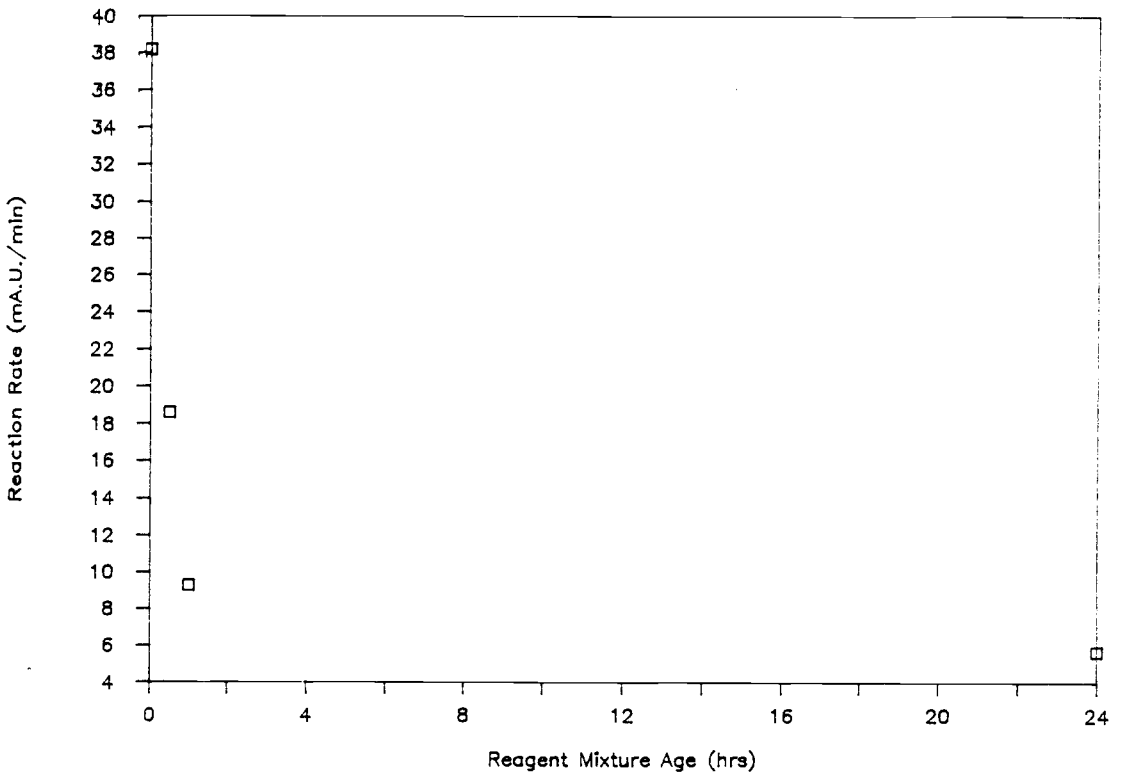

Figure 17. Dependence of reaction rate on the age of reagent mixture. Benzene concentration, 0.01% (v/v).

fluorescent dansyl chloride derivative must be preceded by the chromatographic separation of the derivatized and free dansyl chloride which is also fluorescent.

Another alternative procedure considered involved the coupling of the phenol with a diazotized aromatic amine to form an azo dye which is monitored by absorption at 450 nm (41). This technique also proves unsuitable for in situ analysis because a high pH (11) required for the formation of the azo dye. The high pH allows for the availability of the phenolic anion required for coupling. This pH requirement is not compatible with the acidic environment required for the hydroxylation of benzene using Fenton's reagent (40). Therefore, the two reactions cannot take place simultaneously in the same cell.

CONCLUSIONS

The investigation of derivatization of gasoline and small ring aromatics in aqueous systems has revealed several associated problems. Primarily, this detection scheme is severely limited by the need for a single phase system. Conditions were developed for which the Baudisch reaction does successfully produce aromatic derivatives from benzene and alkyl benzene substrates in a totally aqueous environment but with only limited efficiency. The Baudisch reaction though moderately effective in single phase derivatization is not suited for in situ monitoring for several reasons. First, the lifetime of the mixed reagents is short such that the reagents must be mixed just prior to lowering of the optrode into the sample location or remotely after the optrode is lowered into the sample. A remote addition must include a means of flushing and replenishing spent reagents. Second, the λ_{max} value used in the analysis (310 nm) is relatively short. Even though the absorption wavelength is longer than the native species (the alkyl benzenes), it is still far from the suitable visible wavelength range. A final shortcoming of the modified Baudisch reaction is the lack of formation of a fluorescent species from the analyte which could be detected using optrode designs presently in use.

Even though the Baudisch reaction does not meet the current demands required for in situ fiber optic sensing, the methodology presented in this thesis is suitable for bench top applications. The modified Baudisch reaction may be used to determine alkyl benzene contaminants down to about 0.1 μg/mL levels.

As mentioned above, the need for reagent replenishment in the

modified Baudisch reaction prevents this methodology from being used with most previous developed optrode designs. The second part of this thesis addresses this limitation to in situ analysis by introducing the ability to replenish spent reagent within the optrode.

DEVELOPMENT OF THE REMOTE REACTION CHAMBER FOR FIBER OPTIC SENSING

CONVENTIONAL METHODOLOGY

Kinetics-Based Fluorescence Determination of Aluminum in Aqueous Solution

Aluminum is the most abundant metal in the earth's crust and the third most abundant element. Despite the ubiquitous nature of this metal, relatively little is known about its effects on environmental and human effects while in aqueous solution.

Typical levels of Al^{+3} have been previously reported for natural waters. Al^{3+} concentrations range from 2 to 98 µg/L in freshwater streams and rivers (42, 43) and 0.05 to 5.5 µg/L in coastal seawaters (45-46). Determination of Al(III) at these levels is a challenging analytical problem.

Some of the most common analytical methods currently used for aluminum determinations include flame atomic absorption spectrometry (47), graphite furnace atomic absorption spectrometry (48), ICP atomic emission spectrometry (49). Other methods of detection include the colorimetric ferron (50), aluminon (51, 52), and catechol violet methods (53), and the fluorometric lumogallion method (54, 55). Of these methods none provide both a low detection limit and a convenient methodology to the analyst.

A kinetics-based fluorescence method for the determination of

aluminum in aqueous solution was developed by Campi (7). In this method trace levels of aluminum in water are determined by monitoring the rate of formation of a fluorescent aluminum chelate. The complexing agent used is the dye, 2,4,2'-trihydroxyazo-benzene-5'-sulfonic acid, also known as acid alizarin garnet R (AAGR) or Garnet-Y. The structure of this chelating agent is shown in Figure 18 in both its uncomplexed and its aluminum form.

Several studies and applications of the dye have been presented in the literature (22, 56-59). All of these studies have involved equilibrium-based analysis. The work by Campi is unique in that it involves a kinetics-based technique.

This procedure involved the addition of 2 mL of a standard aluminum solution to a 1-cm pathlength fluorescence sample cell with an Eppendorf automatic pipet. Next 1 mL of a solution of 2.0 M pH 4.75 acetate buffer and 140 mg/L AAGR solution was added by an automatic injecting syringe which initiated the reaction. This provided an in-cell concentration of 47 mg/L for AAGR and 0.67 M for the buffer. The rate was measured over a 16-s period after an 8-s delay time from the injection. The excitation and emission wavelengths were 366 and 570 nm, respectively. The calibration curve was linear over 4 orders of magnitude and a detection limit of 0.1 ng/mL Al^{3+} was calculated. Interference studies showed that the method was very selective.

This methodology developed by Campi provides the analyst with a method that offers a relatively simple reaction scheme and an excellent detection limit and dynamic range. Due to these favorable characteristics, this method of aluminum analysis is easily adapted to a remote sensing application in this thesis.

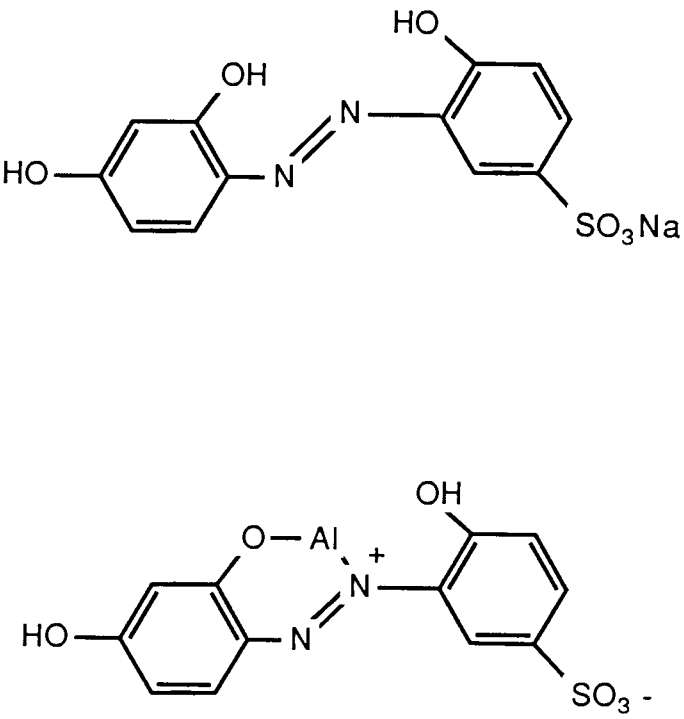

Figure 18. Molecular structure of Garnet-Y (top) and Al-Garnet-Y (bottom).

The Method of Standard Addition

In analytical situations where analyte interferences due to the sample matrix are significant, the method of standard additions is often used. This method provides compensation for nonspectral interferences and certain spectral interferences which may reduce or enhance the analytical signal by a fixed factor independent of the analyte concentration.

A standard addition procedure involves obtaining the analytical signal (S_X) for the sample from a total signal and blank signal measurement. A second solution for analysis is prepared from a volume of sample (V_X) to which a relatively small volume (V_S) of a concentrated solution of the analyte is added. From this mixture a second analytical signal (S_{X+S}) is obtained from the total signal and the blank signal. These data are assumed to fit the following equations

$$S_X = mc_X \tag{2}$$

$$S_{X+S} = m(c_X V_X + c_S V_S)/(V_X + V_S) \tag{3}$$

where m is the slope of the calibration curve. These equations apply if the analytical signal is proportional to the analyte concentration in the sample matrix before and after the addition. The concentration of the analyte in the original sample is determined by solving equations 2 and 3 for c_X or

$$c_X = S_X V_S c_S / [S_{X+S}(V_X + V_S) - S_X V_X] \quad (4)$$

In normal applications of the standard addition method, the volume of the addition standard is much smaller than the volume of the sample ($V_S \ll V_X$). In this case, equation 4 simplifies to

$$c_X = S_X c_S V_S / [(S_{X+S} - S_X)] V_X \quad (5)$$

The basic theory of the method of standard addition is applied to the kinetics-based fluorescence determination of aluminum in water using a unique modification developed in this thesis. This modification is discussed in detail later.

The Determination of Chromium(VI) in Water by Lophine Chemiluminescence

Chromium(VI) levels in natural waters is important to the environmental analyst due to its association with carcinogenic hazards (60, 61). The recommended maximum contamination level (RMCL) in surface waters intended for use as public drinking waters as set by the Safe Drinking Water Act is 0.12 μg/mL (62). Several methods are currently in use which allow for the determination of chromium at this contamination level (63-69). In these methods however, several problems are encountered. These include the distinction between total chromium and Cr(III) or Cr(VI), time consuming sample preconcentration procedures, and extensive sample preparation involving harsh conditions which may change the natural [Cr(VI)] to [Cr(III)] ratio by oxidation

or reduction.

A methodology to determine trace levels of Cr(VI) in water free of these difficulties was developed by Marino in 1981 (70). This chemiluminescence (CL) technique involves observing the base-activated CL of lophine in the presence of hydrogen peroxide which is enhanced by Cr(VI).

Marino's work employs a discrete sampling CL photometer system developed in this lab and described earlier (71). The CL reagents and the sample solution are added to a 1-cm pathlength cell in the photometer as follows. First 1 mL of the Cr(VI) sample is added initially to the cell followed by 0.5 mL of a 0.2 M H_2O_2 solution (cell concentration, 0.04 M). Next 0.5 mL of a 2×10^{-3} M lophine is added into the cell (cell concentration, 4×10^{-4} M) where mixing is accomplished by a magnetic stir bar located in the cell. The three above solutions are added to the optical cell using Eppendorf automatic pipets. Finally 0.5 mL of a 4.0 M KOH (cell concentration, 0.8 M) is injected into the cell with an automatic syringe to initiate the CL reaction. A peak-shaped CL signal is observed with the maximum at about 1 s after injection of the base. This methodology provided a DL of 300 ng/L and found linearity up to 100 µg/L.

The simplicity and performance characteristics of this CL technique are well suited for remote sensing of Cr(VI) as discussed later.

IN SITU TRACE ANALYSIS USING THE REMOTE REACTION CHAMBER

Instrumental

Cell Operation and Design

The design and implementation of the remote reaction chamber (RRC) optrode is unique to this research. The concept arose from the need to develop methodology which would allow remote determination of species which are not detectable by current remote sensing technologies. The idea is to construct a small reaction chamber, into which excitation and emission fibers are inserted, that can be lowered into the sample and which has provisions for drawing in sample, adding one or more reagents, and mixing. This would allow for in situ conversion of the analyte to a luminescent product. The luminescence intensity of this product can be correlated to the analyte concentration after the cell has been calibrated with the appropriate standards.

Several prototypes of an RRC optrode were constructed and tested. Figure 19 shows diagrams of the final design of the RRC used for this research. Through the application of a vacuum across the reaction chamber via the exit port through a one-way check valve, the sample solution of interest is drawn into the chamber through a one-way check-valve and the entrance port. After the reaction chamber has been filled with sample solution, the vacuum is terminated. At this point reagents are injected into the sample through reagent injection lines by an automatic syringe system. The present system is configured to

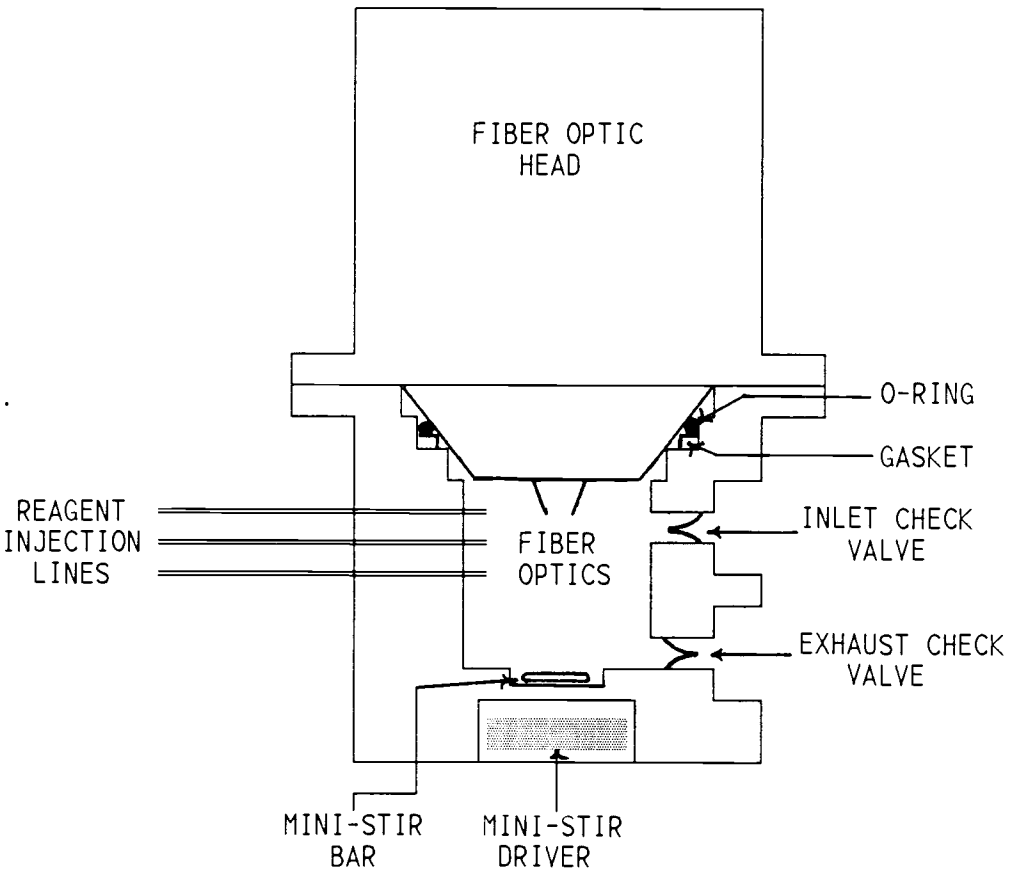

Figure 19a. Drawing of the remote reaction chamber and fiber optic head.

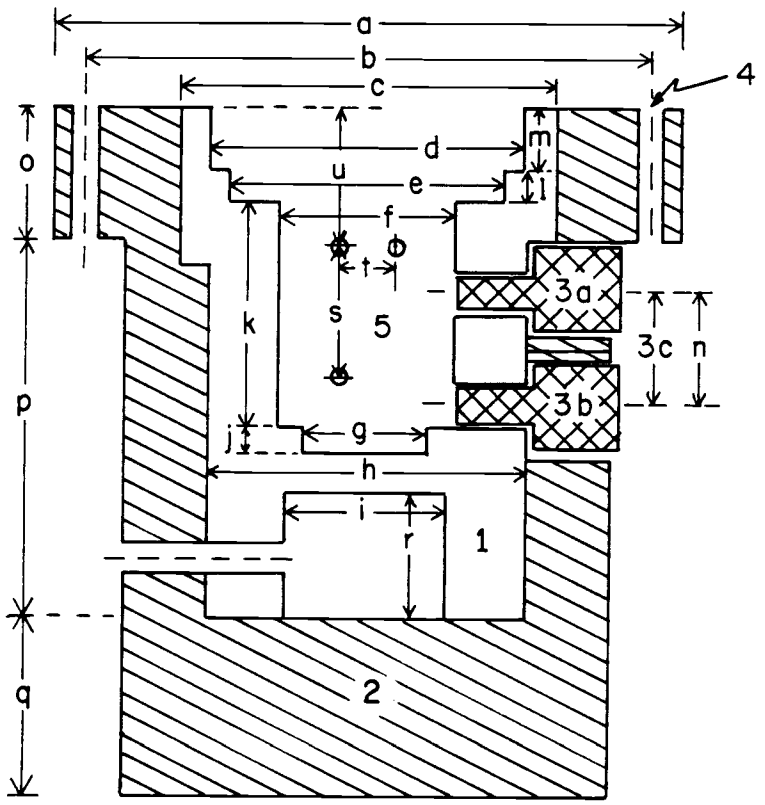

Figure 19b. Schematic of remote reaction chamber for in situ analysis.

Dimensions (all measurements in inches): a, 2.5; b, 2.25; c, 1.50; d, 1.25; e, 1.10; f, 0.71; g, 0.50; h, 1.275; i, 0.65; j, 0.10; k, 0.90; l, 0.15; m, 0.25; n, 0.45; o, 0.50; p, 1.50; q, 0.75; r, 0.50; s, 0.50; t, 0.45; u, 0.60.

Notes: 1, Teflon reaction cell; 2, Delrin outer shell; 3a, Duckbill inlet check valve; 3b, Duckbill exhaust check valve; 3c, Holes drilled in Delrin outer shell for check valves are 0.421 in. Holes drilled in Teflon chamber for check valves are #25 and are tapped 10-32.; 4, 8 #43 drill holes tapped 4-40 are evenly spaced around circumference of Delrin collar.; 5, Reaction chamber reservoir (reagent injection lines enter cell at a 90° angle relative to the intake and exhaust ports). When the fiber optic head is attached, the tips of the optical fibers are 0.78 in from bottom of reservoir.

accommodate up to 3 injection lines. The reagent/analyte mixture is stirred using a miniature Teflon magnetic stir bar (10 mm x 3 mm) and a mini-stir driver (Hellma Cuv-O-Stir model 333) located below the sample chamber in the RRC. If necessary, reaction chamber heating could also be accomplished by using of a small heating coil but was not used in the present model.

The RRC optrode was constructed to use with a fiber optic fluorescence monitoring system developed by Jeff Louch in this laboratory. The components of this system are schematically illustrated in Figure 20. The system includes 75-W Xenon arc lamp source and housing with an elliptical reflector, excitation filter, 600-μm core fused silica excitation and emission fibers, emission monochromator and/or filter, photomultiplier tube (PMT) detector, signal processing electronics, and a digital voltmeter (DVM) and strip chart recorder for signal monitoring. The RRC was designed to mate with the fiber optic head designed by Louch which holds the excitation and emission fibers.

The source radiation is focused on the entrance fiber which transmits the radiation into the coupling chamber. The radiation exiting this fiber passes through an excitation filter and is intercepted by an F/1 collimating lens that is one focal length from the fiber tip. The collimated beam is split by a quartz plate and the reflected beam is monitored as a reference signal by a photodiode (PD). The transmitted beam passes through an F/1 focusing lens and is focused upon the excitation fiber which leads to the RRC. The excitation fiber enters the RRC at an angle of 20° relative to the emission fiber as shown in Figure 19a. The luminescence radiation is

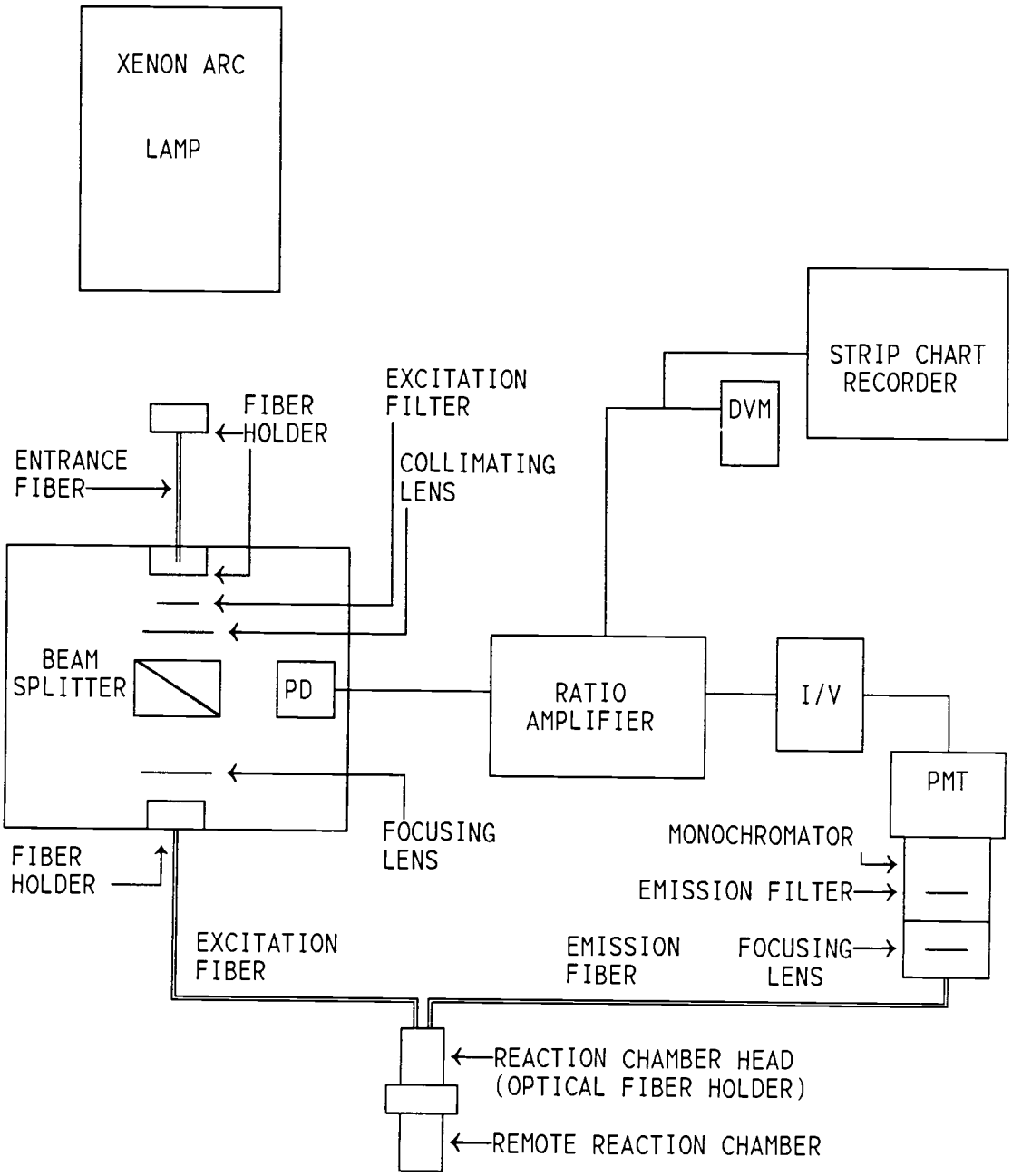

Figure 20. Optical system for fluorescence monitoring of the remote reaction chamber.

collected and transmitted by the emission fiber to the monochromator/ filter and PMT housing. The emission beam is focused on the entrance slit of the monochromator or directly onto the PMT by an F/0.75 focusing lens after it exits the emission fiber. Additional wavelength selection is achieved with an emission filter.

The photodiode unit also contains a current-to-voltage (I/V) converter. The PMT anode is connected to an I/V converter to provide a voltage signal. The feedback resistor and time constant are adjustable. The ratio of the emission signal to the reference signal is taken by an analog voltage divider which compensates for source fluctuations. The divider output is input to the strip chart recorder and DVM for signal monitoring. The compensated fluorescence signal at the divider output can also be monitored through a voltage to frequency converter for microcomputer data processing. The output signal can be processed in either a kinetics-based (slope of initial signal versus time) or equilibrium-based (steady-state luminescence) mode.

RRC Construction

As can be seen in Figure 19b the RRC is constructed in two pieces (excluding valves). The inner chamber is constructed of white Teflon to provide an inert reaction container. The Teflon chamber is inserted into an outer cell of black Delron to provide a light-tight reaction chamber. The miniature stir bar driver is inserted in a machined cavity in the bottom of the Teflon cell.

The fiber optic head of the RRC is made of similar construction with Teflon exposed to the reaction chamber and a Delron outer case.

An air-tight seal between the two pieces of the RRC is achieved using an o-ring (1/8" x 1 1/16") and a flat rubber gasket (1/8" x 1/16" x 1 1/8") which are both shown in place in Figure 19a.

The air-tight seal provided by the o-ring and gasket proved to be critical to the design of the RRC. Initial experimentation with previous RRC designs demonstrated poor volume reproducibility. Different volumes of sample were drawn into the RRC from run to run if the seal was not air tight.

RRC Solution Intake and Waste Valves

Passive one-way check valves (Clippard Minimatic part number MCV-1) were used to control flow of sample solution into and out of the RRC. The valves utilize a rubber duckbill design and have a working range of 0 to 300 psi and open at a cracking pressure of 1/2 psi. Because the valves are constructed primarily of brass, they might be unsuitable for use with highly acidic solutions. However, due to the unavailability of miniature (≤ 1 in.) valves constructed of inert materials such as Teflon, brass valves which measure 0.75 in x 0.375 in were used.

The relative location of the two valves determines the solution volume of the RRC. The cell volume is also dependent upon which valve (upper or lower) is used for the intake and which for the waste. When the lower valve was used as the intake, the solution volume in the RRC varied dramatically offering poor volume precision. Using the upper port as the intake provided reproducible volumes from run to run and was the configuration employed in all further applications of the RRC.

The centers of the valves were place 0.360 in. apart to provide a solution volume of 4.0 mL. This solution volume was determined by first viewing the level to which the cell filled when the vacuum was applied. For viewing, a 150-mL beaker was fitted on top of the lower RRC piece in place of the reaction chamber head. The cell filled to a level just above the upper valve inlet. Later the cell was filled to the same level and then the water was emptied into a beaker and weighed. From the mass of water (4.02 g) and the cell diameter (1.80 cm), the total depth of sample in the cell (excluding the cavity for the stir bar) is calculated to be 1.57 cm.

Reaction chamber rinsing is accomplished by the continuous application of vacuum across the reaction chamber. The chamber may be rinsed with the solution to be analyzed or with rinse solution as needed. Solution flow through the reaction chamber is ≈2 mL/s which provides thorough rinsing of the Teflon chamber in approximately 30 s.

Reagent Injection Lines

A diagram of the injector and vacuum system used is presented in Figure 21. Reagents are introduced to the cell through 0.042 in id Teflon tubing (Hamilton). These reagent lines are friction fitted to provide an air-tight seal into 0.060-in drill holes in the RRC wall. These lines are fitted flush with the inside wall of the reservoir. For the aluminum studies, the upper two injector lines were employed, while in the chromium study, all three lines were used. Injection of reagent solutions is controlled by Hamilton syringe injector systems. The volume delivered is controlled by the size of the syringe installed

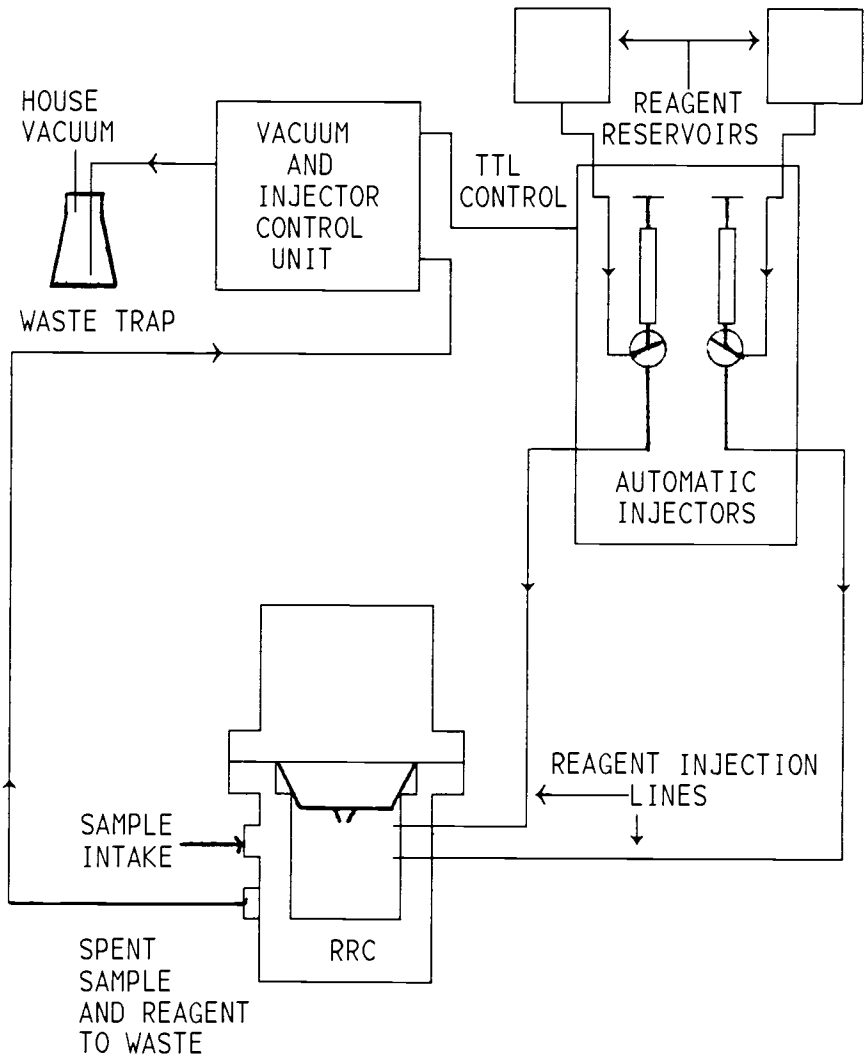

Figure 21. Schematic of injector and vacuum system for sample and reagent addition and cell flushing.

and adjustment of the distance that the syringe plunger travels. For the aluminum study, a dual syringe injector fitted with two 1-mL syringes was used (part # 77100). This same dual syringe injector and a single syringe injector (part # 77000) with a 1-mL syringe were used in the chromium determination. The Hamilton injectors also allow for control of the speed of reagent addition as needed for the specific application. The pneumatic Hamilton injectors operate on house air pressure (≤30 psi) and provides automatic injection and syringe refill via an external reagent reservoir.

The dual and single Hamilton syringe injectors were previously modified by Dewald (72) and Marino (70), respectively, for TTL control of their operation. For each injector, a solid state relay (SSR) and 2 3-way pneumatic air valves are attached to the back of the injector casing. The common ports of the 3-way valves are attached to the two sides of the pneumatic piston that drives the syringe. The switched ports of the 3-way valves are attached to house air. When a 0-V signal is applied to the control input of the SSR, the 3-way valves are in their normally closed position and air pressure is applied to the side of the syringe drive piston that pushes the syringe plunger toward the syringe needle. In this position a 3-way solution control valve directs solution flow from the syringe to the reagent injection line. A 5-V control signal causes 115 V ac to be applied to the coils of the 3-way valves and switches the valves to their normally open position. Air pressure is applied to the other end of the syringe drive piston and simultaneously to the 3-way solution control valve. The solution control valve rotates to allow solution from the reagent reservoir to enter the syringe as the syringe plunger pulls back from the needle

under the applied air pressure. When the 5-V signal is turned off, the valves return to the positions described above and the reagent is injected into the cell.

The control signal to the dual injector is supplied by a vacuum and injector control unit. This box houses a 9-V battery, a divider, a push button switch, a toggle switch, a SSR 3-way air valve and a 2-way vacuum control valve. When the button is pushed, a 5-V signal is sent to the SSR on the syringe injector. The syringe(s) fill during application of this signal. When the button is released, the solution in the syringe is injected into the reagent lines.

The toggle switch on the control box is used to apply a 5-V signal to the control box SSR which controls the 3-way valve located in the control box. When the 5-V signal is applied to the control box SSR, the 3-way valve switches to its normally open position and house air is directed to and opens the 2-way vacuum control valve. The 2-way valve is located between the exhaust port line of the RRC optrode and a waste trap which is connected to house vacuum. During the period the SSR is activated, sample is pulled through the RRC optrode and is collected in the waste trap.

For the single syringe injector (not shown in Figure 21), a push button and battery fitted to the injector body operate the injector.

RRC Modifications For CL Analysis

For CL studies the excitation (not in use) and emission fibers were covered with black heat shrink tape to prevent light leaks through the fiber cladding. Light entering around the RRC fittings was blocked

by wrapping the RRC and fittings with black electrical tape.

EXPERIMENTAL

Aluminum-AAGR Study

Solution Preparation

All aqueous solutions used in RRC experimentation were prepared with MP water (described earlier). Glassware used was rinsed initially with a 50/50 (v/v) HNO_3 and MP water mixture and then with MP water.

For the aluminum determination, a 100 mg/L Al^{3+} solution was prepared by diluting 1.2367 g of $Al_2(SO_4)_3$ (Fisher Scientific) and 3 mL of reagent grade HNO_3 (Allied Chemical) with MP in a 1000-mL volumetric flask. All other aluminum standards were prepared as dilutions of the 100 mg/L solution and were also made acidic with 3 mL of HNO_3. All aluminum solutions were prepared under a forced air clean hood in volumetric flasks designated for the specific concentrations of aluminum. A 9 M buffer solution was prepared by mixing 515 mL of acetic acid (Baker) and 300 mL of water, adjusting to pH 4.75 by the addition of 10 M NaOH (Mallinckrodt), and diluting to 1 L. A 0.564 g/L AAGR (Berncolors-Poughkeepsie) solution was also prepared.

For the determination of aluminum in tapwater a water sample was obtained from a laboratory faucet after letting the water flow for 15 min. The water sample was analyzed immediately without further treatment.

Analysis Procedure

The aluminum solutions were aspirated into the reaction chamber of the RRC optrode by applying house vacuum as described earlier. For convenience a section of Teflon tubing was connected to the inlet port of the RRC. The opposite end of this tubing was placed in a volumetric flask containing the test solution. This tubing can be easily removed to allow insertion of entire RRC into the sample pool as needed. Reaction chamber rinse and spent solutions are drained via this same vacuum system which contains an in-line solution trap.

The analysis solution is aspirated into the reaction chamber for approximately 30 s to thoroughly rinse the chamber. After termination of the vacuum, the cell volume is allowed to equilibrate for a minimum of 5 s before reagent injection.

For this study 0.5 mL of the buffer solution and 0.5 mL of the AAGR solution provided in-cell concentrations of 0.90 M and 56 mg/L, respectively, for the two reagents (total cell volume of 5 mL). Initially the injections were accomplished simultaneously using the pneumatic, dual syringe Hamilton auto-injector via 2 separate injection lines. These injection lines are orientated to direct the reagents directly into the sample at a level close to the distal end of the fiber in the RRC (Figure 19). The syringe volumes were adjusted to 0.5 mL and the air pressure of the injector was set to yield an injection time of ≈0.5 s. In later studies, the reagents were mixed in equal volumes before injection of 1 mL by a single Hamilton syringe.

The excitation wavelength range was determined by an interference filter (peak wavelength of 480 nm and a 20-nm half-width). The

emission monochromator was set to 585 nm with 1-mm square entrance and exit slits yielding a spectral bandpass of 20 nm. A 530-nm cutoff filter was also used in front of the PMT to reduce the background signal.

The initial rate was estimated as the slope of the emission signal from the time of reagent addition to 1 min after injection as recorded on the strip chart. All measurements were conducted with a PMT voltage of 700 V, and a 1-s time constant. The feedback resistance was varied from 0.1 to 100 MΩ as required to maintain the signal within the full scale limit of the strip chart recorder.

Analysis Procedure for the Method of Standard Addition

As described earlier a single reagent line may be used to inject a AAGR and buffer solution mixture. This leaves a second reagent injection line to be used for analyte addition.

To accommodate the additional volume of the added analyte in the RRC, the delivery volume of the AAGR/buffer injection syringe was decreased from 1 mL to approximately 0.5 mL to maintain a total cell volume of 5 mL as used in all applications of the RRC. This decrease in volume provides an in-cell concentration for AAGR and buffer of 28 mg/L and 0.45 M, respectively. The effect of this decrease in reagent concentration is considered later in this thesis.

The second reagent injection syringe was adjusted to deliver 0.5 mL of analyte standard to the RRC. A 1000 ng/mL Al^{3+} standard was used for all standard addition data presented. All other analysis parameters used in the standard addition application remained the same

as those presented in the previous section.

Reagent Solution Cleanup

To decrease the metal ion contamination in the acetate buffer, an ion-exchange resin purification was conducted as previously described (70, 73). Polypropylene ion exchange columns (Bio Rad #731-1110, 0.7 cm x 4 cm) were inserted into the mouths of 100-mL polypropylene bottles with the bottoms removed and assembled with a heat gun. Approximately 20 mL of wet 100-200 Chelex-100 resin was poured into two identical columns. One column was suspended over the other to facilitate double treatment of the solution.

The buffer and the AAGR solutions were passed through two separate column pairs. The AAGR solution underwent a significant color change from orange-red to a dark red-black. This color change was not mentioned in the previous work by Campi (7).

Determination of Chromium (VI) by Lophine Chemiluminescence

Solution Preparation

Solutions were prepared in clean glassware with MP water as previously described. Reagents for the CL determination of Cr(VI) in water were prepared as follows to provide reagent concentrations in the reaction cell similar to those found to be optimum for the reaction by Marino (8).

Standard Cr(VI) solutions were prepared by serial dilution from a

1000 mg/L stock solution. This stock solution was prepared by dissolving 2.7258 g $K_2Cr_2O_7$ primary standard (G. Frederick Smith Chemical). Before weighing this standard was dried at 105° C for 1 hr and cooled. A 4.0 x 10^{-3} M lophine (2,2,4-triphenylimidazole) (Aldrich Chemical) was prepared by dissolving 0.3020 g of lophine in 25 mL of 2 M HNO_3 and then diluting to 250 mL with reagent grade methanol (J. T. Baker). A standard solution of 0.4 M hydrogen peroxide was prepared by diluting 45.4 g of stabilized H_2O_2 (Spectrum Chemical) to 1 L in 0.01 M ethylenediaminetetraacetic acid (EDTA) (Anachem). An approximately 8 M potassium hydroxide solution was also prepared by dissolving 449 g of KOH (J. T. Baker) in 1 L water.

Analysis Procedure

To allow for the addition of the third reagent (KOH), an additional reagent injection line was added to the RRC. The position of this new injection line relative to the other injection lines is discussed later.

The injection sequence for the reagents is as follows. The sample is aspirated into the cell as previously described. The H_2O_2 and lophine stock solutions are both added in 0.5 mL aliquots via separate injection lines. This injection provides in-cell concentrations of 0.4 M in H_2O_2 and 4 x 10^{-4} M in lophine. This reaction mixture is allowed to mix for 15 s followed by the initiation of the CL reaction by the injection of 0.5 mL KOH stock (cell concentration, 0.8 M). The peak-shaped CL signal is recorded on a strip chart recorder for analysis. To facilitate collection of the entire luminescence signal

transmitted by the emission fiber, the monochromator and emission filter were removed. This enables the collected signal to be focused directly on the face of the PMT with minimum signal attenuation. The PMT voltage was 800 V and the feedback resistance was varied between 0.1 and 100 MΩ as required to maintain the signal within the full scale boundaries of the recorder.

Solution Concentrations for Comparison Study

In the comparison study of the collection efficiency of the discreet sample CL and the RRC CL cell, the concentrations of reagents and sample remained constant. This was achieved by injecting 0.25 mL of each reagent solution (the H_2O_2, KOH, and lophine solutions described above) into the discreet sample cell (1-cm pathlength)which contained 2 mL of sample. All solutions except the KOH were delivered using Eppendorf automatic pipets. Note that all volumes are one-half of those used for the RRC optrode. The KOH solution was delivered with the single injector automatic syringe.

RESULTS AND DISCUSSION

Investigation of the Kinetic-Based Determination of Aluminum in Water Using the RCC OPTRODE

Analytical Wavelength Selection

To determine the optimum excitation wavelength for the monitoring of the Al-AAGR complex, the absorption spectra of the complex and AAGR were obtained and are shown in Figure 22. The absorption spectrum of Al-AAGR complex shows a maximum at 476 nm. A 480-nm interference excitation filter was used for all studies because it closely matches this absorption maximum.

In the work by Campi, an excitation wavelength of 366 nm provided the maximum fluorescence signal for the Al-AAGR complex because the Xe-Hg arc lamp has a strong Hg emission line at this wavelength. This excitation wavelength is at an absorption minimum for the Al-AAGR complex (see Figure 22). For the fiber optic system excitation at 480 nm rather than 366 nm provides a greater signal for the Al-AAGR chelate because the absorptivity of the complex and the excitation radiant power are greater than those at 366-nm with a Xe arc lamp.

Figure 23 is the emission spectrum of Al-AAGR complex obtained with the Varian SF 330 spectrofluorometer using an excitation wavelength of 476 nm. The spectrum shows a maximum emission band at 560 nm.

The wavelength setting of the emission monochromator in the fiber optic system (Figure 20) was varied with a test solution that

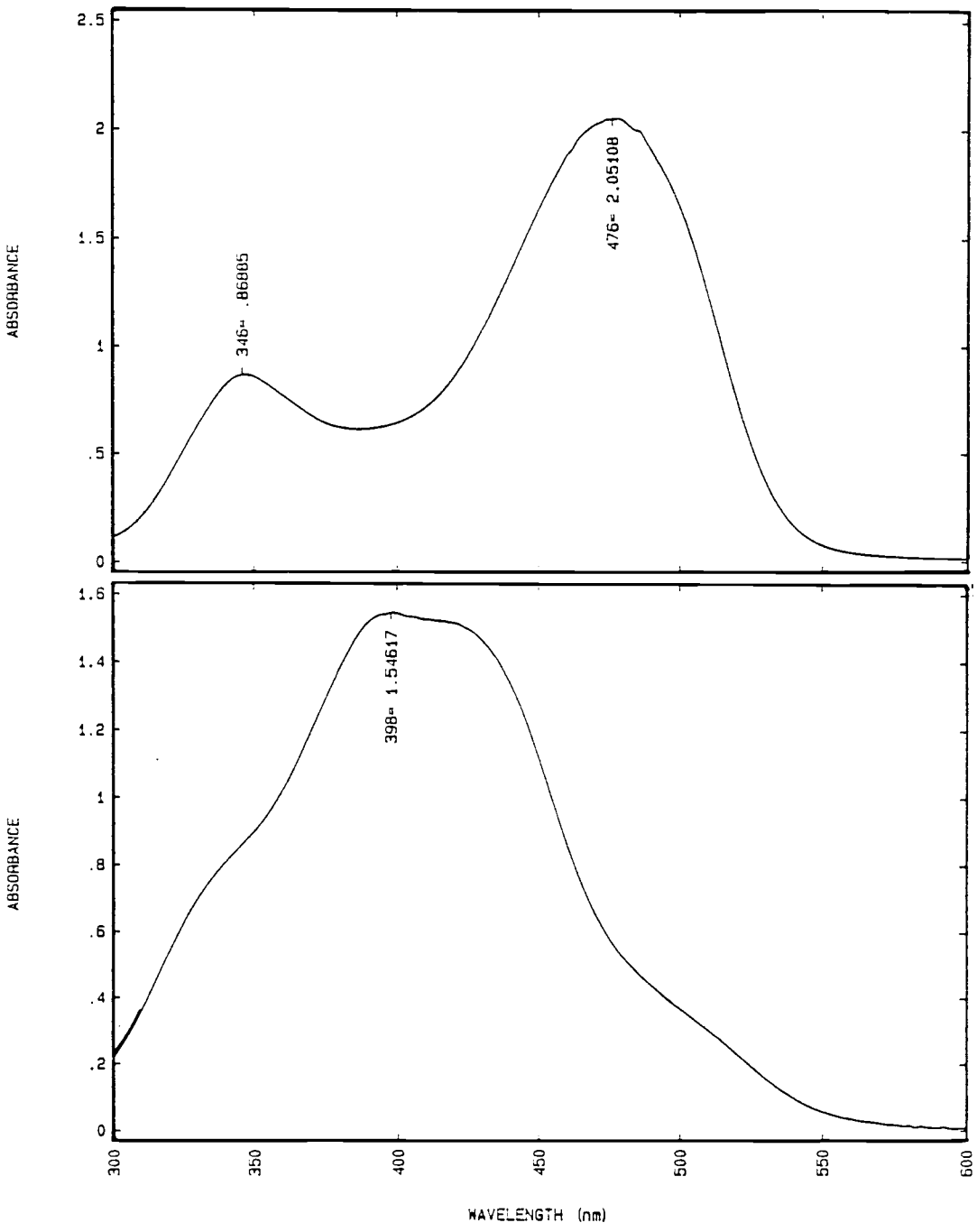

Figure 22. Absorption spectra of AAGR (bottom) and the Al-AAGR chelate (top). Al^{3+}, 83 ng/mL; AAGR, 47 µg/mL; buffer, 0.17 M; 2-nm bandpass.

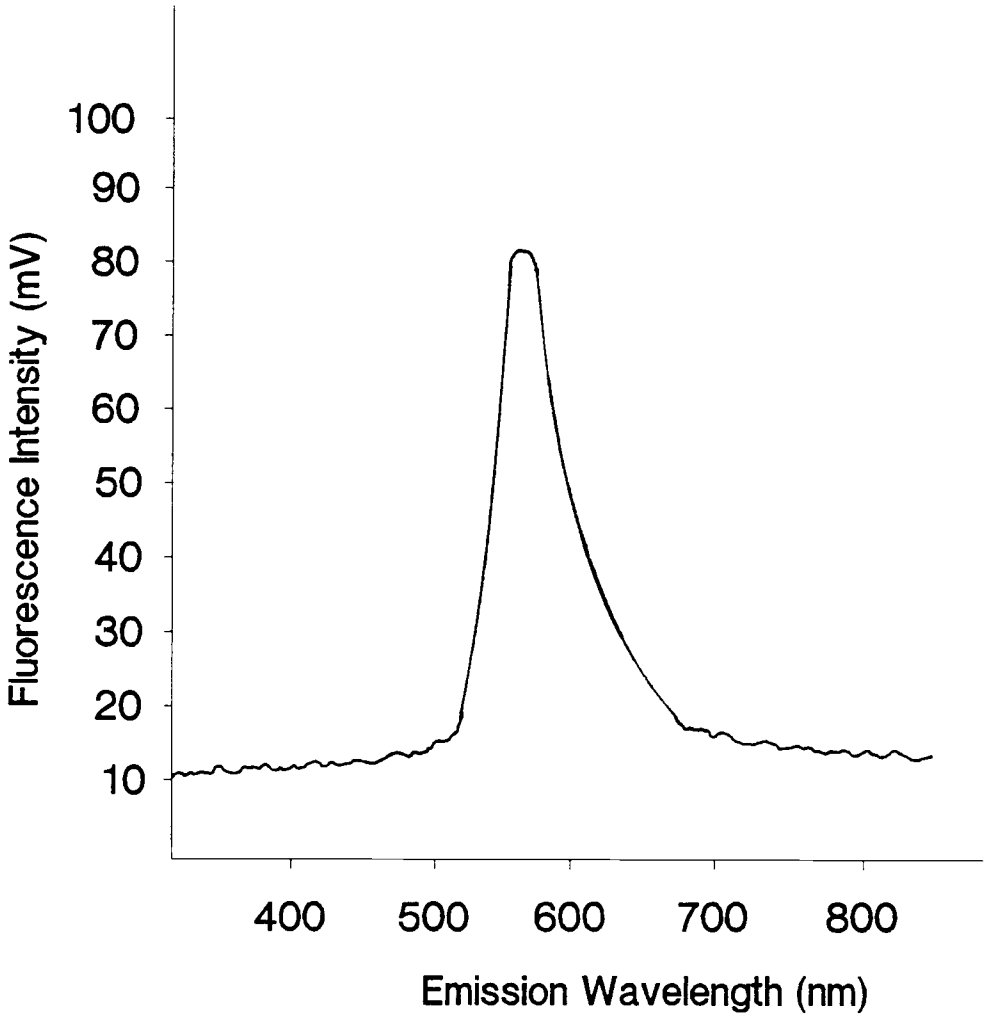

Figure 23. Emission spectrum of the Al-AAGR chelate. λ_{ex}, 480 nm; emission and excitation bandpass, 5 nm; Al^{3+}, 83 ng/mL; AAGR, 47 µg/mL; buffer, 17 M.

provided a steady state emission signal for Al-AAGR complex (a 100 mg/L Al^{3+} solution that had been allowed to reach equilibrium). The maximum emission signal was observed at 577 nm and was chosen as the emission monochromator wavelength setting for all further studies of the Al-AAGR system.

Buffer and Garnet-Y Solution Cleanup

As shown by Campi (7), the control of the reaction mixture pH is critical in the Al-AAGR system for kinetics-based measurements. The acetic acid and sodium hydroxide used in this buffer potentially contain metal contamination which would lead to a high blank signal in the analysis. As discussed in the experimental section, the buffer was cleaned using a Chelex-100 resin to remove trace levels of interfering ions. Table XII lists the signal to background ratio (S/B) obtained with both cleaned and uncleaned buffer. The cleaned buffer system offers a better S/B by a factor of 18 and therefore was used in all further studies.

The pH of the cleaned buffer was determined to be 4.83 which is 0.08 higher than the uncleaned buffer. This small change in buffer pH did not significantly affect the reaction rate of the Al-AAGR system, and therefore the pH was not adjusted further.

The AAGR solution was also cleaned with the Chelex-100 resin as was outlined in the experimental section. The treated AAGR solution was red-black as compared to the red-orange color of the uncleaned AAGR. When tested for reactivity in the kinetics-based determination of aluminum, the treated AAGR proved inactive. Hence, all further

Table XII. Buffer Solution Clean-up[a]

Treatment	Blank Corrected Analyte Rate (mV/min)	Blank Rate (mV/min)	S/B
None	10	72	0.14
Chelex Resin	63	24	2.6

[a]All blank rates are averages of 10 measurements and all analyte rates are the average of 5 measurements. R_f, 100 MΩ; C_f, 0.01 μF; Al^{3+}, 1 ng/mL; AAGR, 56 mg/L; buffer, 0.9 M. Buffer and AAGR solutions were injected separately for mixing in the cell and in-cell concentrations are reported.

studies were conducted using cleaned buffer and uncleaned AAGR.

Injection of Mixed and Separate Buffer and AAGR-Y Solutions

Two procedures for introducing the reagents to the reaction cell were compared. The first involved injecting the reagents separately and the second involved premixing equal volumes of the reagents before injection.

In theory, premixing the reagents would allow formation of the Al-AAGR complex from trace levels of aluminum contamination in the reagents. The formation of the Al-AAGR complex would lead to a greater initial background signal level upon addition of the mixed reagents to the sample, but the blank rate should be smaller since the product has already formed.

The theory is supported by the data presented in Table XIII where the blank rates and their relative standard deviations are reported. With separate injection of the reagents, the blank rate is a factor of 1.5 times greater than that with injection of the mixed reagent. A rapid initial rise (30- to 40-mV) is observed upon reagent injection with the mixed reagent system due to the background fluorescence from the Al-chelate formed in the reagent mixture. The response curves for the blank signals for both reagent injection modes as well as the response curve with mixed reagents for 1 ng/mL Al^{3+} are shown in Figure 24. The initial rapid rise in signal was not used in determining the initial rate for the mixed reagent system. Because the mixed reagent injection offers a slightly better S/B and better precision in the analyte rate as shown in Table XIII, it was used for

Table XIII. Comparison of Mixed and Separate Reagent Systems

Method	Blank Rate[a] (mV/min)	Std. Dev. (mV/min)	Analyte Rate[b] (mV/min)	Std. Dev. (mV/min)	S/B
Mixed	19	4.1	61	1	4.3
Separate	28	3.1	59	5.5	2.1

[a]Blank rates are the mean of 10 measurements.
[b]Analyte concentration was 1 ng/mL. Analyte rates are the mean of 5 measurements.

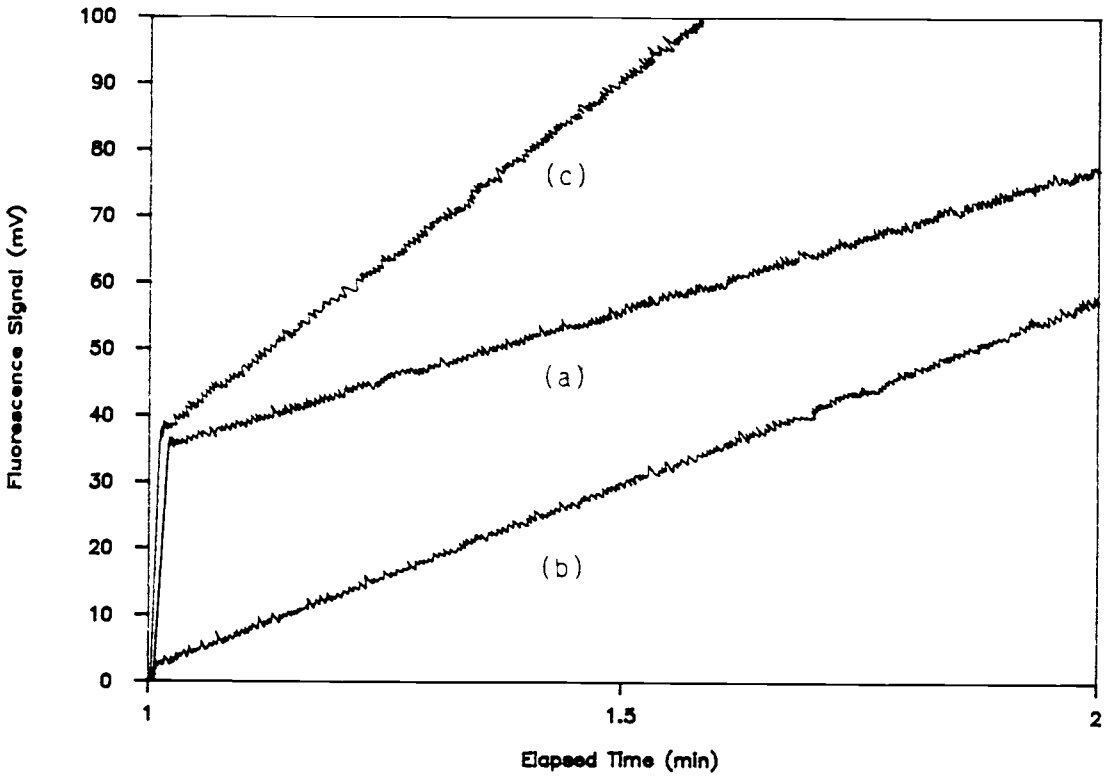

Figure 24. RRC optrode blank response curves for mixed (a), separate (b) reagent systems and the response curve for 1 ng/mL Al^{3+} (c) using the mixed reagent system.

further studies. Moreover, use of a single injection line simplifies the system and allows the flexibility of using the second injection line for standard addition of the analyte which is discussed later.

Calibration Curve

A calibration curve for the Al-AAGR system utilizing the RRC optrode is presented in Figure 25. The data used in Figure 25 are provided in Table XIV along with precision data for the experiment.

From the ratio of two times the blank noise (Table XIV) to the slope of the linear calibration plot (61.3 mV/min/(ng/mL)), the DL for aluminum is calculated to be 0.13 ng/mL. This value compares well with the 0.12 ng/mL DL determined by Campi in the bench top analysis using the Al-AAGR system (7).

A laboratory tap water sample was analyzed for its aluminum concentration from the signal obtained (Table XIV) and the slope of the calibration curve. An aluminum concentration of 43 ng/mL was obtained.

The data in Table XIV demonstrate good linearity up to 100 ng/mL Al^{3+}. The deviation from linearity is 13% for the 1000 ng/mL standard and 63% for the 10,000 ng/mL standard. Deviations are probably due to inner-filter effects. The RRC optrode provides a linear response to Al^{3+} in water using the Al-AAGR system for over four orders of magnitude. Again the RRC operation compares well with the bench top application which provides a dynamic range of over four orders of magnitude.

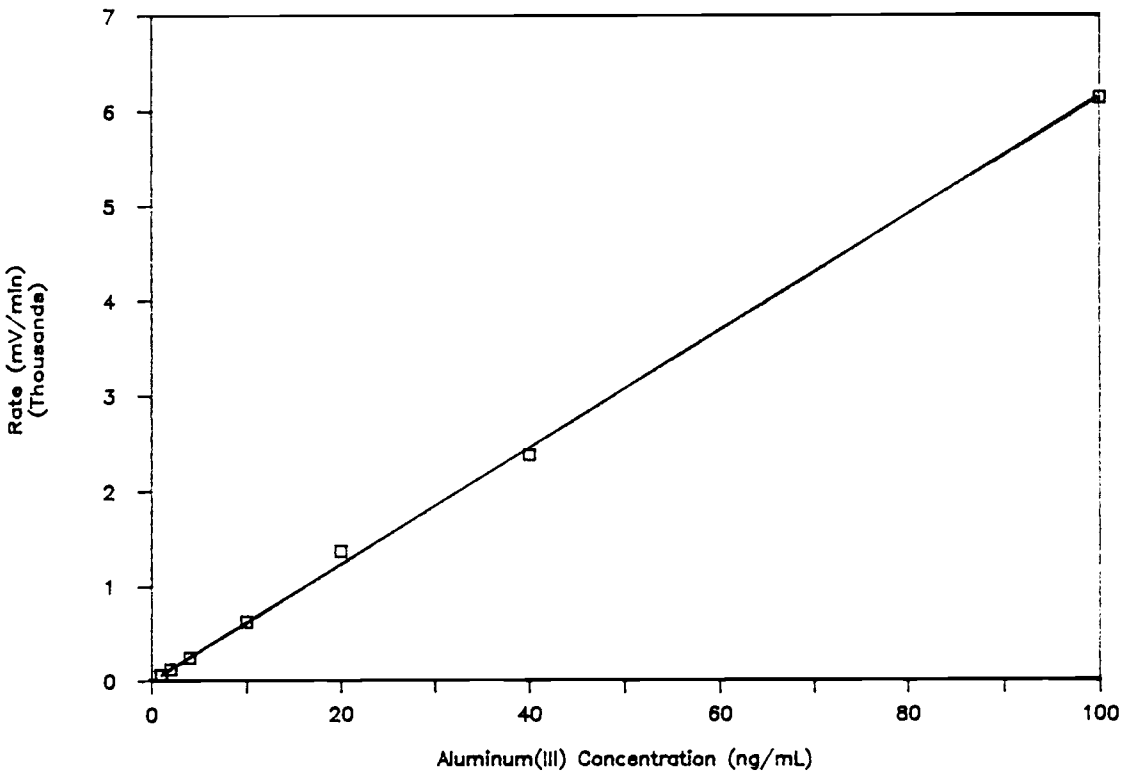

Figure 25. Calibration curve for Al^{3+} from 0 to 100 ng/mL. All data points are blank corrected. Regression line is plotted as a least squares fit.

Table XIV. Calibration data for the determination of Al^{3+} in water using the RRC optrode[a]

Al^{3+} (ng/mL)	Mean Rate (mV/min)	Std. Dev. (mV/min)	RSD (%)	Blank Corrected Rate (mV/min)
0.0	19	4	21	0.0
1.0	80	1	1	61
2.0	143	7	5	124
4.0	264	5	2	245
10	647	5	1	628
20	1390	12	1	1371
40	2400	28	1	2380
100	6150	50	1	613
1000	5.30×10^4	1.2×10^3	2	5.30×10^4
10000	2.23×10^5	8.6×10^3	4	2.23×10^5
Tap Water	2.57×10^3	58	2	2.55×10^3

[a]For n = 5 for Al^{3+} standards and n = 20 for the blank.

Application of the Method of Standard Addition

The analysis parameters set as optimum for the determination of aluminum by the kinetics-based fluorescence reaction using the RRC optrode remained unchanged for the standard addition study except for the decrease in the volume of the AAGR/buffer solution. On a molar basis, 28 mg/L AAGR is 1.2×10^{-4} M and a 1 μg/mL Al^{3+} is 3.7×10^{-5} M (3.0×10^{-5} M in cell). Thus the chelating agent is present in excess of Al^{3+} by a factor of 4. Hence, the slight decrease in AAGR concentration the reaction mixture does not significantly affect the rate observed.

To insure that the proper pH was maintained in the reaction chamber after the addition of acidified samples, the pH of the spent reaction solutions was monitored. After several determinations of Al^{3+} concentrations in samples acidified to pH 2, the reaction chamber was disassembled and the solution pH was determined with a pH meter. In all cases the spent solution pH was between 4.65 and 4.80 which is a favorable pH range for this reaction.

In applications of the method of standard addition, the accuracy and precision of reagent and sample volumes are of considerable importance in obtaining accurate results (equation 4). If the volume of the addition standard is much smaller that the sample volume, the analyte concentration in the unknown may be determined without considering these volumes (equation 5). For standard addition conditions used, a relatively large volume of the analyte standard is injected (0.5 mL). This volume is 11% of the sample volume and cannot be neglected. Moreover, the sample is mixed with 0.5 mL of reagent.

To correct for these volume changes, the volumes of the addition standard, reagents, and sample must be known with high accuracy.

To compensate for these complications, a modified method of standard addition was developed which does not require that all volumes be accurately known. This modified method initially requires the measurement of the rate for six conditions in the RRC optrode. These six measurements are obtained as follows. Initially a blank solution (MP water) is aspirated into the RRC. To this solution additional blank is injected via the analyte standard injection line followed by signal measurement (S_1). This signal is used in blank correction of the analyte and standard addition signals. A second signal is obtained from the blank (aspirated as sample) and addition of a 1000 ng/L Al^{3+} addition standard (S_2). The third measurement is obtained from an aspirated standard with a known analyte concentration (100 ng/mL) which is injected with blank solution (S_3). Next the rate of the same known aspirated analyte sample injected with the addition standard is obtained (S_4). The fifth and sixth measurements are of the sample of interest injected with blank (S_5) and sample injected with the addition standard (S_6). The rates obtained using the RRC optrode for these six conditions are presented in Table XV.

To correct for the volume changes in the cell, the signal from the sample is taken as the rate measured after dilution of the sample of volume V_x by a volume of reagent V_r and a volume of blank equal to the volume of standard injected (V_s). In this case

$$S_x = mV_xc_x/V_f \qquad (6)$$

Table XV. Standard addition data obtained with the RRC optrode

Measurement #	Sample (ng/mL)	Addition Standard	Signal (mV/min)	Std. Dev.[a] (mV/min)	RSD (%)
1	Blank	Blank	26	3.8	1
2	Blank	1000 ng/mL	1493	41	3
3	100 ng/mL	Blank	1150	50	4
4	100 ng/mL	1000 ng/mL	2612	48	2
5	Tap Water	Blank	383	6	2
6	Tap Water	1000 ng/mL	1780	29	2

[a]Blank-blank data are the average for n = 20, all other data are averages for n = 5. Data are reported without blank-blank correction.

where $V_f = V_X + V_S + V_r$.

The signal obtained after injection of volume V_S of the addition standard in the sample and volume V_r of reagent is

$$S_{X+S} = m(c_X V_X + c_S V_S)/V_f \tag{7}$$

Solving equations 6 and 7 for c_X yields

$$c_X = (S_X c_S V_S)/[(S_{X+S} - S_X)V_X] \tag{8}$$

or

$$c_X = S_X c_S'/(S_{X+S} - S_X) \tag{9}$$

where c_S' is the adjusted concentration of the injected standard in the sample mixture ($c_S' = c_S(V_S/V_X)$).

To use equation 9, c_S' is experimentally determined as follows. The calibration slope m' is obtained from the blank-corrected rate for a standard of analyte concentration c_{st} substituted for the sample or

$$m' = (S_3 - S_1)/c_{st} \tag{10}$$

The adjusted concentration for the injected standard is next obtained from the blank-corrected rate for injection of the addition standard into a blank or

$$c_s' = (S_2 - S_1)/m' \qquad (11)$$

From the data in Table XV, m' = 11.24 mV/min/(ng/mL) and c_s' = 130.5 ng/mL. From the nominal volumes, c_s' was expected to be 1000 x 0.5/4.0 = 125 ng/mL.

To verify the procedure, the blank-corrected rates for the 100 ng/mL standard, $(S_3 - S_1)$ and $(S_4 - S_1)$, are used for S_X and S_{X+S}, respectively, in equation 9. The value of c_X determined is 100.3 ng/mL which is in very good agreement with the expected value of 100.0 ng/mL.

For the tapwater sample, the Al^{3+} concentration calculated from $(S_5 - S_1)$ and the calibration slope is 31.8 ng/mL. From $(S_5 - S_1)$, $(S_6 - S_1)$, and equation 9, the Al(III) concentration is calculated as 33.3 ng/mL. These two concentrations differ by only 4.8%. The results indicate there are no serious interferences in the tapwater sample that alter the rate of the analytical reaction or affect the fluorescence signal from the Al^{3+} complex.

These results demonstrate, for the first time, that in situ standard addition can be applied to remote fiber optic fluorescence measurements. Standard addition compensates for interferences in the sample which affect the analytical signal obtained for a given concentration of analyte. Moreover, compensation is provided for other factors such as excitation source intensity or the transmission characteristics of the fibers which can change with time.

In this study, blank and standard addition solutions were injected through the same injection line after proper flushing. For routine applications it would be possible to employ separate blank and standard

addition lines and arrange for the same injection volume for both solutions. Alternatively, it would be possible to calculate all sample, standard addition, and reagent volumes and use appropriate equations to calculate the analyte concentration (c_x) in the sample.

The Determination of Chromium(VI) by Lophine Chemiluminescence Using the RRC Optrode

Dark Current Signal

The shielding of the fibers and of the RRC and fittings as discussed in the instrumental section, reduced the background signal observed significantly due to leakage of room light. A low background signal is extremely important in CL measurements due to the high PMT gains which must be used to amplify the weak CL signals for detection. Because no wavelength selection device, such as a bandpass filter is used, to monitor the CL, stray light entering the cell is also viewed at all wavelengths. The light-tight integrity of the RRC was verified by observing the dark current signal with the overhead lights on and off at night. This observation showed little or no fluctuation in dark current signal or noise with changing external light levels and thus indicates the modified RRC provides an analysis environment suitable for CL measurements.

Reagent Injection Lines and Viewing Fiber Locations

The dependence of the CL signal on the location of the emission

fiber tip was studied. This was accomplished by inserting the fiber 0 (fiber tip just inside body of RRC head) to 35 mm into the RRC. At each fiber location, the position of the KOH injection line was also varied among the three available reagent injection sites. Neither the position of the fiber or of the KOH injection line had a significant effect on the CL signal observed with a 10 µg/mL Cr(VI) test solution. For all further studies the emission fiber was inserted 13 mm beyond the RRC head and the lower injection line position was used for KOH injection.

Calibration Curve

A calibration curve for the lophine CL determination of Cr(VI) in water is presented in Figure 26. The data used in the construction of this curve are also provided in Table XVI. The curve shows that the CL determination for Cr(VI) using the RRC is linear in response from 0 to 10 µg/mL. A typical CL response curve is shown in Figure 27.

No blank signal was observed and the DL was therefore calculated as twice the dark current noise (1/5 of the peak-to-peak dark signal, 3 mV) divided by the slope of the calibration curve (555 mV/(µg/mL)) to be 11 ng/mL. This DL is about 37 times worse than the 0.3 ng/mL DL reported by Marino (70) but still considerably less than the 120 ng/mL specified by the safe water drinking act. This loss in detectability is discussed in further detail below.

A laboratory tapwater sample was analyzed for its Cr(VI) content using the RRC. The sample was found to be free of chromium contamination at the levels detectable by this methodology. When 900

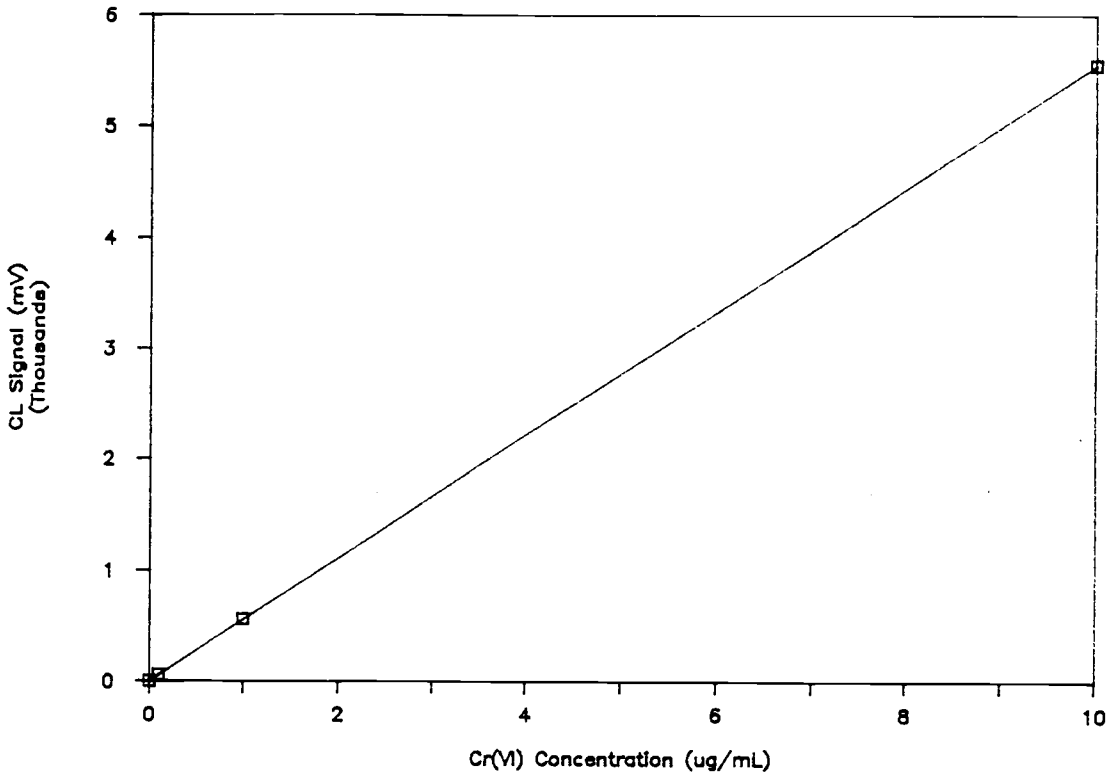

Figure 26. Calibration curve for Cr(VI) determination using the RRC fiber optic system.

Table XVI. Cr(VI) CL data obtained using the RRC and the discrete sampling photometer

Cr(VI) (μg/mL)	Instrument (PMT)	Signal (mV)	Std. Dev. (mV)	RSD (%)
0.1	RRC (4840)	56	5.6	10
1.0	RRC (4840)	558	10	1.8
10.0	RRC (4840)	5.55×10^3	50	1.0
100	RRC (4840)	1.85×10^4	100	0.5
1.0	RRC (1P28)	153	7.6	5.0
1.0	Discrete[a] Sample (1P28)	2.08×10^3	29	1.3
Tapwater	RRC (4840)	< 10		
1.0	Submerged RRC (4840)	550	10	1.8

[a]DL for discrete sample system is calculated to be 3 ng/mL

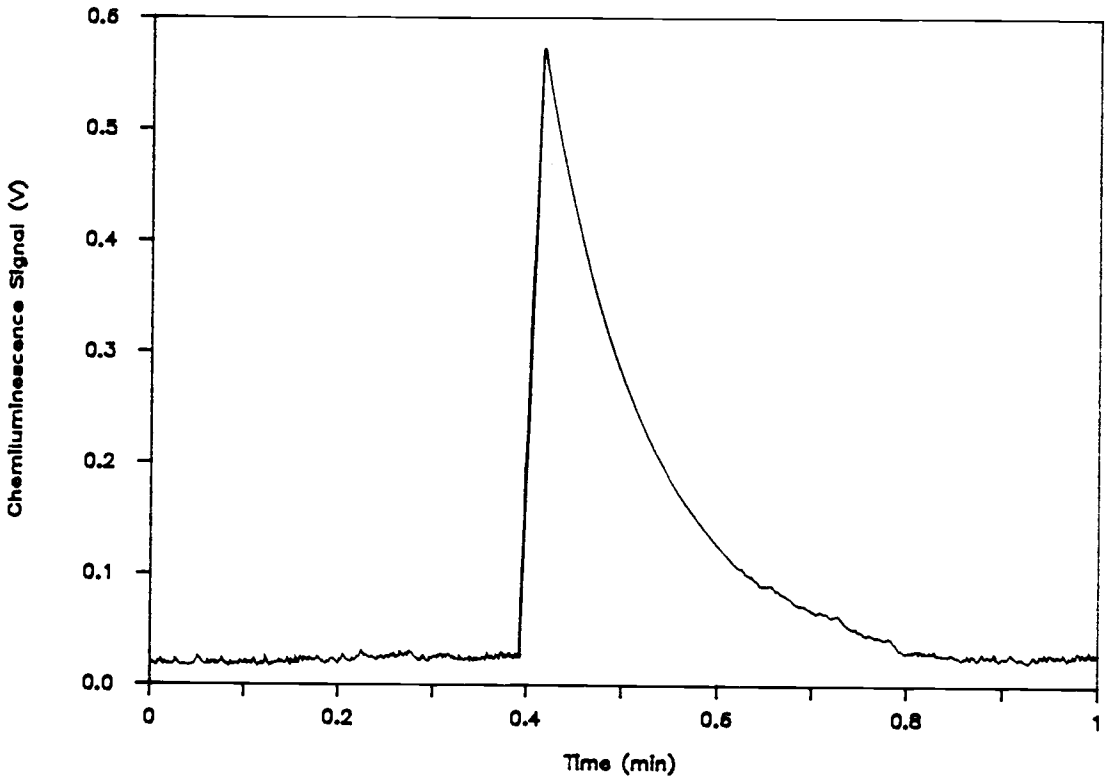

Figure 27. Chemiluminescence response curve for for 1 μg/mL Cr(VI). The feedback resistance was 100 MΩ.

mL of the tapwater sample was spiked with 100 mL of a 10 µg/mL Cr(VI) standard to give a 1.0 µg/mL Cr(VI) concentration in the sample, a recovery of 97% was achieved.

RRC Optrode Submersion Study

In order to verify the RRC optrode operation as a submersible unit, experimentation was completed where the entire RRC was submerged in a large container which held an aqueous solution of 1 µg/mL Cr(VI). The data obtained in these experiments is provided in Table XVI. The data indicates that the RRC functions equally well submerged as it does when a remote sample is introduced via an inlet line.

Collection Efficiency Comparison

The collection efficiency of the CL fiber optic system was compared to that of the discrete sampling CL photometer used by Marino (70). The same PMT and signal processing components were used with both instruments so that the measured CL signal was directly proportional to the light levels incident on the detector. The same PMT voltage and feedback resistor were also used for both sets of measurements. Also the volumes were adjusted so that the in-cell concentrations of Cr(VI) and all reagents were equivalent for both systems. The PMT used in this experiment (RCA 1P28) was different than the one used in the previous RRC experiments (RCA 4840) including the Cr(VI) determination discussed above.

The data collected in this experiment are presented in Table XVI.

These data show that the fiber optic RRC system collects approximately 14 times less CL signal than does the discrete sampling photometer. The collection efficiency of the optrode system is less because the 600-μm diameter fiber views CL from only a small solution volume element.

The detection limits for Cr(VI) with the discrete sampling and RRC systems were 3 ng/mL and 39 ng/mL, respectively. The peak-to-peak dark noise for the 1P28 PMT was 15 mV. The DL with the 1P28 PMT for the RRC system is about 3 times worse than that obtained with the 4840 PMT. The difference in detection limit for the RRC system with the 4840 PMT and that obtained by Marino is due both to differences in collection efficiency and differences in the cathodic responsivity and dark current noise characteristics of the PMT used.

CONCLUSIONS

A new optrode for use in remote sensing applications has been described which allows in situ mixing of the sample and one or more reagents to produce a luminescent species. Innovations in optrode design presented here permit the use of bench top chemistry for in situ applications. The design also makes it possible for the first time to apply the method of standard additions to remote sensing using fiber optic sensors.

The analytical application of the RRC optrode was first demonstrated using a kinetic method for the determination of aluminum based upon the formation of a fluorescent chelate of aqueous aluminum with AAGR. In this application the utility of the RRC optrode was characterized by a low detection limit of 0.13 ng/mL Al(III) and a linear response of over four orders of magnitude. This range encompasses aluminum concentrations found in most natural water samples. This determination was conducted using external calibration standards.

In a second application it was demonstrated that the RRC optrode was uniquely suited to implement the method of standard additions in remote sensing analysis. An experimental design is presented which uses modified standard-addition equations and measurements to provide an accurate and precise determination of Al(III) at trace levels. The standard-addition method eliminates the need for external calibration of the RRC optrode. Also the method of standard additions can provide compensation for multiplicative matrix interferences or differences in the values of experimental variables (e.g., excitation radiation

intensity, temperature) that occur between the time of calibration with external standards (usually before the optrode is deployed) and sample measurements. These attributes of the RRC optrode greatly increase the flexibility of its use as a remote sensing device.

The application of the RRC in the determination of aqueous Cr(VI) demonstrated that this optrode is suitable for chemiluminescence analysis. A detection limit of 11 ng/mL and a linear response up to 10 µg/mL was achieved. Given that the recommended maximum contamination level for drinking water is 120 ng/mL Cr(VI), the RRC optrode seems a viable methodology for environmental monitoring of this metal.

The RRC optrode developed in this research is based on a simple and logical design and offers a favorable new approach to the area of remote chemical sensing devices. The applications presented in this thesis represent only a small fraction of the possible applications of the RRC optrode. The success of the studies presented here indicate that further research of the analytical utility of the RRC optrode for detecting other species of interest is warranted.

FINAL CONCLUSIONS

This work has involved two distinctly different approaches to remote sensing of chemical contaminants in aqueous systems. In the initial study presented in this thesis, the analysis of water samples for trace levels of gasoline and small ring aromatics proved a difficult task. It was demonstrated, given the current available designs of remote chemical sensors, that in situ derivatization of small ring aromatics into species suitable for remote detection is very difficult. The product of the Baudisch reaction absorbs in the UV where attenuation by optical fibers would be excessive. Also the reagents can be mixed only immediately prior to the analysis. However, this initial work did demonstrate the usefulness of the Baudisch reaction for determining small ring aromatics and gasoline in water by a bench-top kinetics spectrophotometric analysis procedure.

The second approach to remote sensing applications resulted in greater success. The RRC optrode was presented as an alternative to current optrode designs providing the options of multiple reagent addition, stirring, and possibly heating. These options provide added versatility and selectivity in conducting remote sensing.

Most importantly, the RRC optrode design allows in situ mixing of the sample with two or more reagents. This allows many existing chemical derivatization schemes to be employed for remote sensing. Most optrode designs are based on reactions involving one reagent or a mixed reagent system that is immobilized or held in a reservoir at the optrode tip. The RRC optrode can be used for chemical systems requiring multiple reagents where the reagents cannot be premixed due

to instability. Moreover, the reagent system is totally replaced for each determination.

Another critical advantage of the RRC optrode design is the ability to carry out standard additions. For most current optrode designs, the calibration response of the optrode must be determined with external standards before the optrode is deployed (e.g., lowered into the groundwater through a well). To provide accurate results, all factors that affect the calibration response must be the same for the samples and standards. Clearly this is difficult to achieve. In-situ standardization does compensate for some matrix interference effects and variations in the magnitude of experimental values.

The current design of the RRC optrode does limit the analyst to methods of detection involving production of a luminescent species by reaction of the analyte with appropriate reagents. It is feasible to modify the first generation RRC optrode so that other types of spectrochemical detection, such as absorption, could be conducted. For spectrophotometric detection the RRC design could be modified to incorporate mirrors into the cell to reflect incident radiation through the solution contained in the cell and back to the fiber connected to the detection system. The greater attenuation of currently available optical fibers at shorter wavelengths does however limit the use of the RRC optrode to analysis in the visible region of the electromagnetic spectrum with conventional sources. This limitation was a key factor that prevented the development of a remote detection scheme for gasoline in water. The RRC optrode design presented here addresses specifically the problem of loss of reactivity of mixed reagent systems such as that encountered in the gasoline study.

In final conclusion, it has been shown that the RRC optrode is a viable new technology made available for future research in the area of remote sensing. The RRC optrode provides a tool to solve many problems encountered in current remote sensing technologies.

BIBLIOGRAPHY

1. Seitz, W. R., Anal. Chem. 1984, 56, 16-34A.

2. Maugh, T. H., Science 1982, 218, 875-876.

3. Chabay, I., Anal. Chem. 1982, 54, 1071-1080A.

4. Wolfbeis, O. S., Pure and Appl. Chem. 1987, 59, 663-672.

5. Arnold, S. M. (ed.), Talanta 1988, 35, #2.

6. Angel, S. M., Spectroscopy 1987, 2, #4, 38-48.

7. Campi, G. L., "A Reaction Rate Determination of Aluminum With a Microcomputer Based Spectrofluorometer", MS Thesis, Oregon State University, (1982).

8. Marino, D. F.; Ingle, J. D., Jr., Anal. Chem. 1981, 53, 455-458.

9. Lane, J. C., "Gasoline and Other Motor Fuels", ECT 2nd ed., vol. 11, pp. 652-695 (1978).

10. Peter, F. M., (Editor), "The Alkyl Benzenes", National Academy Press, Washington D. C., 1981.

11. Savage, P., Chemical Week 1986, Sept. 24, 11-12.

12. Miller, R. L., J. Chromatogr. 1983, 264, 19-32

13. Matisova, E., J. Chromatogr. 1984, 303, 151-163.

14. Sanders, W. N., Anal. Chem. 1968, 40, 527-535.

15. Brooks, K., Chemical Week 1986, Sept. 24.

16. Dumas, A., Nat. Pet. News, January 1980.

17. Kramer, W. H., Groundwater Pollution From Gasoline, Groundwater Monito. Rev. 1982, 2(2), 18-22.

18. Osgood, J. O., Hydrocarbon Dispersion in Groundwater, Groundwater 1974, 12(6), 427-438.

19. Williams, D. E., Gasoline Pollution of a Groundwater Reservoir, Groundwater 1971, 9(6), 50-56.

20. Fyrit, P., Quantitatine Determination of Petroleum Hydrocarbons in Water by IR Spectroscopy, Vodni Hospod., B 1978, 28 (3), 77-81.

21. Tamaka, T.; Ichimura, K., The Determination of Oil in River Water by IR Absorption Spectroscopy, Nara-ken Eisei Kenkyusho Nenpo 1980, 15, 56-61.

22. Guilbault, G. G., Practical Fluorescence, Marcel Dekker, New York, 80-82 (1973).

23. Chudyk, W. A., Anal. Chem. 1985, 57, 1237-1242.

24. Chudyk, W. A., Adv. in Instr. 1986, 41(3), 1237-43.

25. Kochi, J. K., Free Radicals, Vol. 1, Wiley and Sons, New York, 1973, 629-631.

26. Silverstein, R. M., Bassler, G. C., Morrill, T. C., Spectrometric Identification of Organic Compounds, 4th Ed., Wiley and Sons, New York, 305-331 (1984).

27. Jefcoate, C. R. E.; Smith, J. R., Norman, R. O. C., JCS (B) 1969, 1013-1017.

28. Williams, A. T. Rhys, Fluorescence Detection in Liquid Chromatography, Perkin-Elmer, Buckinghamshire, England, 1980, 46-60.

29. Cassidy, R. M., J. Chromatog. 1972, 72, 85-89.

30. Baudisch, O., JACS 1941, 63, 672-677.

31. Kazuhiro, M.; Iwao, T.; Ruozo, G., Tet. Let. 1966, 47, 5889-5891.

32. Kazuhiro, M., JOC 1967, 32, 2516-2519.

33. Cronheim, G., JOC 1947, 12, 1-6.

34. Maruyama, K.; Tanimoto, I., JOC 1967, 32, 2516-2520.

35. Maruyama, K.; Tanimoto, I., Tet. Let. 1966, 47, 5889-5892.

36. Stein, G.; Weiss, J., Nature 1948, 161, 650-656.

37. Stein, G.; Weiss, J., Nature 1950, 166, 1104-1110.

38. Milas, N. A., JACS 1937, 59, 2342-2344.

39. Milas, N. A., JACS 1937, 59, 2345-2347.

40. Walling, C., JACS 1978, 100, 4814-4818.

41. Ratanathanawangs, S. K.; Crouch, S. R., Anal. Chim. Acta 1987, 192, 277-287.

42. Burrous, W. D., Aquatic Aluminum: Chemistry, Toxicology, and Ennvironmental Prevalence, Critical Reviews of Environmental Control 1977, 7, 136-140.

43. Sorenson, T. R.; Campbell, I. R.; Tepper, L. B.; and Lingg, R. D., Environmental Health Perspectives 1974, 8, 3-95.

44. Hydes, D. T., Nature 1977, 268, 136-140.

45. Hydes, D. T.; Tiss, P. S., Science 1977, 7, 755-759.

46. Atkinson, L. P.; Stefanson, U., Geochim. Et Cosmochin. Acta 1969, 33, 1449-1452.

47. Powell, W. A., Anal. Chem. 1953, 25, 960-964.

48. Playle, R.; Gleed, T.; Jonasson, R., Anal. Chim. Acta 1982, 134, 396-373.

49. Allain, P.; Mauras, Y., Anal. Chem. 1979, 51, 2089-2092.

50. Driscoll, C. T.; Baker, J. P., Nature 1981, 284, 161-165.

51. Hach Chemical Company Instruction Pamplet, Aluminum Method Using Alu Ver III Aluminum Reagent for Water, Hach Chemical Company, Ames, Iowa, 1981.

52. Shull, K. E., J. Amer. Water Works Assn. 1960, 52, 779-783.

53. Hunter, J. B.; Ross, S. L., Water Pollution Control 1980, 79, 413-417.

54. Haugen, G. R.; Steinmetz, L.L., Appl. Spec. 1981, 35, 568-571.

55. Hydes, D. T.; Tiss, P. S., Analyst 1976, 101, 922-927.

56. White, C. E.; Hoffman, D. E.; Magee, T. S., Jr., Spectrochimica Acta 1957, 9, 105-112.

57. Fletcher, M. H., Anal. Chem. 1960, 13, 1822-1827.

58. Fletcher, M. H., Anal. Chem. 1960, 13, 1827-1836.

59. Powell, W. A., Saylor, T. H., Anal. Chem. 1953, 25, 960-964.

60. Nau, V.; Nieman, T. A., Anal. Chem. 1979, 51, 424-428.

61. Steig, S.; Nieman, T. A., Anal. Chem. 1978, 50, 401-404.

62. Fed. Regist., 1985, 50, No. 46936.

63. Gilbert, T. R.; Clay, A. M., Anal. Chim. Acta 1973, 67, 289-295.

64. Thompson, K. C.; Wagstaff, K., Analyst 1979, 104, 224-231.

65. Pankow, J. K.; Janauer, G. E., Anal. Chim. Acta 1974, 69, 97-104.

66. Felman, F. J.; Knoblock, E. C.; Purdy, W. C., Anal. Chim. Acta 1967, 38, 489-497.

67. Agterdenbos, J.; Van Brockhaven, L.; Jute, B. A.; Shuring, J., Talanta 1972, 19, 341-345.

68. Lovett, R. J.; Lee, G. F., Anal. Chem. 1976, 10, 67-71.

69. Gosink, T. A., Anal. Chem. 1975, 47, 165-168.

70. Marino, D. F., "Analytical Chemiluminescence Measurements and Instrumentation", PhD Thesis, Oregon State University (1980).

71. Hoyt, S. D.; Ingle, J. D., Anal. Chem. 1976, 48, 232.

72. Dewald, R. L., "A Microcomputer Automated Anodic Stripping Voltametric Analysis for Trace Heavy Metal Speciation", PhD Thesis, Oregon State University (1984).

73. Separating Metals using Chelex 100 Chelating Resin, Product Information 2020, Bio-Rad Laboratories, Inc., Richmond, CA, (1981)